

Modeling the Formation of Giant Planet Cores I: Evaluating Key Processes

Harold F. Levison

Southwest Research Institute

1050 Walnut St, Suite 300

Boulder, CO 80302

hal@boulder.swri.edu

Edward Thommes

Department of Physics

University of Guelph

Guelph, Ontario, N1G 2W1

Canada

and

Martin J. Duncan

Department of Physics

Queen's University

Kingston, Ontario, K7L 3N6

Canada

Received July 15, 2009; accepted December 9, 2009

ABSTRACT

One of the most challenging problems we face in our understanding of planet formation is how Jupiter and Saturn could have formed before the solar nebula dispersed. The most popular model of giant planet formation is the so-called *core accretion* model. In this model a large planetary embryo formed first, mainly by two-body accretion. This is then followed by a period of inflow of nebular gas directly onto the growing planet (Pollack et al. 1996). The core accretion model has an Achilles heel, namely the very first step. We have undertaken the most comprehensive study of this process to date. In this study we numerically integrate the orbits of a number of planetary embryos embedded in a swarm of planetesimals. In these experiments we have included a large number of physical processes that might enhance accretion. In particular, we have included: 1) aerodynamic gas drag, 2) collisional damping between planetesimals, 3) enhanced embryo cross-sections due to their atmospheres, 4) planetesimal fragmentation, and 5) planetesimal driven migration. We find that the gravitational interaction between the embryos and the planetesimals lead to the wholesale redistribution of material — regions are cleared of material and gaps open near the embryos. Indeed, in 90% of our simulations without fragmentation, the region near that embryos is cleared of planetesimals before much growth can occur. Thus, the widely used assumption that the surface density distribution of planetesimals is smooth can lead to misleading results. In the remaining 10% of our simulations, the embryos undergo a burst of outward migration that significantly increases growth. On timescales of $\sim 10^5$ years, the outer embryo can migrate ~ 6 AU and grow to roughly $30 M_{\oplus}$. This represents a largely unexplored mode of core formation. We also find that the inclusion of planetesimal fragmentation tends to inhibit growth except for a narrow range of fragment migration rates.

Subject headings: planets and satellites: formation

1. Introduction

It is ironic that the most massive planets in the Solar System had to have formed in the least amount of time. Jupiter and Saturn, for example, which are made mainly of hydrogen and helium, must have accreted this gas before the solar nebula dispersed. Observations of young star systems (e.g., Haisch, Lada & Lada 2001; see Hillenbrand 2008 and references therein for a recent review) show that gas disks, at least insofar as they are traced by the presence of dust in the inner AU as well as accretion onto the star, have lifetimes of $\sim 1 - 10$ Myr. So, the gas giant planets had to form before this time. In contrast, the Earth most likely took at least 60 Myr to fully form (based on cosmochemical constraints; Halliday 2004, Touboul et al. 2007; and numerical modeling; Chambers & Wetherill 1998; Agnor, Canup, & Levison 1999), and may have taken as long as 100 Myr.

Thus, one of the most challenging problems we face in our understanding of planet formation is how Jupiter and Saturn could have formed so quickly. In the core accretion model, which envisions that a large planetary embryo formed first by two-body accretion followed by a period of inflow of gas directly onto the growing planet (Mizuno et al. 1978; Pollack et al. 1996), the main difficulty is in the first step. The accretion of a massive atmosphere requires a solid core $\sim 10 M_{\oplus}$ in mass (Mizuno 1980; Pollack et al. 1996; Hubickyj et al. 2005). As we describe in detail below, assembling such a large body, it turns out, offers some serious challenges to the theory of planet formation as it currently stands. The difficulties are threefold: First, the accretion process has to be efficient enough to concentrate such a large mass in (at least) one single body. Second, everything has to happen fast enough ($\lesssim 10^7$ yr, for reasons described above) that when the putative core is ready, there is still enough gas—of order several hundred M_{\oplus} —left in the nearby part of the disk to furnish its envelope. The final problem concerns migration due to planet-disk tidal interactions, which threatens to drop core-sized bodies into the central star faster than they

can accrete (Ward 1986; Korycansky & Pollack 1993; Ward 1997).

In the last five years or so, there has been a concerted effort by the planet formation community to overcome these problems. Indeed, several new ideas have been presented in the literature (see the review in §2 below). However, many of these ideas have yet to be fully explored with modern dynamical simulations. Thus, here we present a series of direct numerical N -body simulations intended to explore these ideas. In particular, we employ a simplistic set of initial conditions that are designed to study the effectiveness of various physical processes rather than realistically model the growth of giant planet cores. This paper is organized as follows. After our review in §2, we describe our numerical methods in §3, our results in §4, and conclude in §5.

2. A Not-So Brief Review of Core Accretion Models

Perhaps the best known simulations of the core accretion scenario are those of Pollack et al. (1996, see Hubickyj, et al. 2005 for an updated version of these models). These simulations follow the growth of a single isolated embryo as it first accreted neighboring planetesimals, and then nebular gas. Although these models show that there are reasonable conditions under which it is possible for Jupiter and Saturn to form in less than 10 Myr, they employed a simplistic model of solid body accretion. Indeed, these models are 1-dimensional and only mimic the dynamical evolution of the system using crude expressions for dynamical stirring and the evolution of the surface density of the planetesimals. As we now describe, more realistic dynamical models fail, in general, to form cores large enough to undergo significant gas accretion before the nebula disperses.

Studies of terrestrial planet formation have shown that solid body growth can occur in three stages. In the first stage, planetesimals grow by runaway accretion, wherein

the largest bodies grow the fastest (Wetherill & Stewart 1989). For the minimum-mass solar nebula (hereafter MMSN, Hayashi 1981) Ida & Makino (1993) argued that runaway accretion stops at a protoplanet mass of only $\sim 10^{-6} M_{\oplus}$.

In the middle stage, known as the ‘*oligarchic regime*’, accretion changes from runaway to self-regulating, as the largest bodies become big enough to gravitationally “stir their own soup” of planetesimals (Ida & Makino 1993, Kokubo & Ida 1998, 2000, Thommes, Duncan & Levison 2003, hereafter TDL03). In this phase, the largest few objects at any given time are of comparable mass, and are separated by amounts determined by their masses and distances from the Sun. As the system evolves, the mass of the system is concentrated into an ever-decreasing number of bodies of increasing masses and separations. This stage ends at a given location in the disk when the local “oligarchy” of largest bodies reach their *isolation mass* (at least within a factor ~ 2), meaning that they have consumed all planetesimals within their gravitational reach. In the terrestrial planet region, typical disk models produce isolation masses of only about Mars mass, thus a third stage must take place in which these bodies’ orbits cross and they collide to form Earth- and Venus-mass bodies.

In the Jupiter-Saturn region, our current understanding is that the first and second stages occurred, but it is possible that the final stage did not. There are two arguments for this. First, in the terrestrial region the last stage of planet formation takes 30 – 50 Myr years in the standard gas-free model (Chambers & Wetherill 1998; Agnor, Canup, & Levison 1999; Chambers 2001), which implies that it should take at least an order of magnitude longer in the Jupiter-Saturn region because of lower densities and longer orbital periods. This is much longer than the lifetime of the gas disks. Second, while the isolation masses in the terrestrial zone are much smaller than the observed planets, in the Jupiter-Saturn region the isolation mass can be roughly what is needed for gas accretion ($\sim 10 M_{\oplus}$), if one were to

accept a significantly enhanced disk mass (Lissauer 1987). Thus, oligarchic growth could, in principle, suffice to produce the giant planet cores.

During oligarchic growth, the planetary embryos enhance their mass by sweeping up much smaller planetesimals, although occasional mergers between embryos do occur (see Thommes & Duncan 2006, hereafter TD06, for a review). The rate of growth is determined by the local surface density of planetesimals, Σ_m , and the random velocities of both the embryos and the planetesimals. The embryos are self-excited, while they are being damped by dynamical friction with the planetesimals. Since during oligarchic growth the overall density of the embryo population is small compared to that of the planetesimal disk, dynamical friction dominates and the embryos are on circular, co-planar orbits. In this case, Kokubo & Ida (1998) show that the embryos are well separated from one another such that $\Delta a = b r_H$, where $r_H = a (M/3M_\odot)^{1/3}$ is the Hill radius of the protoplanet, a is heliocentric distance, and b is a constant with a value of $\sim 5 - 10$.

The planetesimals' random velocities in the oligarchic regime are dominated by stirring due to the protoplanets (indeed this is how this regime is defined). In most of the work that has been done (see below for more detail), it is assumed that this is balanced by the aerodynamic drag due to the nebular gas. One can estimate the resulting equilibrium RMS eccentricity by equating the timescales for these two effects. It is found that $e_m \propto M^{1/3} r^{1/5} \rho_{\text{gas}}^{-1/5}$, where ρ_{gas} is the local density of the nebula, and r is the radius of a typical planetesimal. Note that the embryo growth rate is $\propto \Sigma_m e_m^{-2} \propto \Sigma_m r^{-2/5} \rho_{\text{gas}}^{2/5}$, and thus the dynamically *colder* the system of planetesimals (i.e. the smaller e_m), the faster the embryos grow. Keeping the system cold is key to growing the cores before the nebular gas disappears. This can only happen if the drag forces are large, which, in turn, implies that ρ_{gas} needs to be large and r small.

But, there is a price to be paid for large drag forces. In addition to damping

eccentricities, aerodynamic gas drag extracts energy from planetesimal orbits (Adachi et al. 1976). Indeed, with the balance between damping and gravitational stirring by the protoplanets maintaining a nonzero equilibrium planetesimal random velocity, there is a continuous net orbital decay of planetesimals. The surface density of planetesimals thus changes at a given radius not just because planetesimals are swept up by protoplanets, but also because of this migration. This can have a serious negative effect on the growth of the embryos.

TDL03 studied this in detail using both analytical analysis and numerical N -body experiments. They find that gas drag acts as a two-edged sword in the accretion of massive bodies: On the one hand, increasing the strength of gas drag (by increasing the gas density, decreasing the planetesimal size, or a combination thereof) damps random velocities more strongly and speeds the accretion rate. On the other hand, as also found by Inaba & Wetherill (2001), stronger gas drag also increases the rate at which Σ_m is depleted by planetesimal orbital decay; this causes growth to stall earlier than we might otherwise expect. In particular, assuming a characteristic planetesimal size of 10 km, TDL03 found that in order to produce $10 M_\oplus$ protoplanets in the Jupiter-Saturn region requires a very massive disk (~ 10 times the MMSN). Such a large disk is difficult to reconcile with other constraints, such as those derived from the migration of Uranus and Neptune (Hahn & Malhotra 1999; Gomes, Morbidelli, & Levison 2004). The good news is, however, that the time to reach $10 M_\oplus$ at 5 AU is short, roughly 1 Myr. Decreasing the characteristic planetesimal size decreases the mass at which growth stalls.

Unfortunately, there is more bad news: TDL03 did not include the effects of fragmentation, which leads to considerably less optimistic results. Fragmentation reprocesses a large fraction of the planetesimals to much smaller size, which makes the above problem even worse. The dynamical regime we are considering — wherein the

random velocities of the planetesimals are determined by stirring from much larger bodies — makes it likely that fragmentation will play a role, since planetesimals will collide with relative velocities much larger than their surface escape velocities. Inaba & Wetherill (2001) studied this effect using a statistical rather than an N -body code. They found that the largest protoplanet produced has a mass of less than $2 M_{\oplus}$! This result is thus worrisome for the core accretion model.

In recent years there have been several papers that suggest promising avenues for solving weaknesses in the oligarchic growth model for giant planet core accretion. They include:

- *The role of embryo atmospheres*: The model of Pollack et al. (1996) for the accretion of giant planet cores also models the slow accretion of a gas atmosphere onto a growing giant embryo, prior to the final runaway gas accretion phase. This atmosphere acts to enhance the capture cross-section for additional planetesimals, but because they assume planetesimal sizes of 1-100 km, the tenuous atmosphere present during the initial solids-dominated accretion phase does not play a very large role in raising the accretion rate. However, as a planetesimal's size is decreased, the strength of gas drag it feels is increased. So too, therefore, is its capture radius with respect to a embryo possessing a gas atmosphere. Inaba & Ikoma (2003), hereafter II03, study the capture of planetesimals in the atmosphere of a growing core. Using a simple 1-dimensional numerical model they show that, as long as random velocities of the planetesimals are small compared to the escape velocity from the core's surface, the effective cross-section of the embryos is significantly increased. This can lead to a substantial increase in accretion rate.

Using a Monte Carlo technique, Inaba, Wetherill & Ikoma (2003; hereafter IWI03) studied core formation with fragmentation, radial migration, and gas-enhanced

capture cross-sections. They found that the inclusion of embryo atmospheres effectively rescues the core-accretion model from the perils of fragmentation. The important point is that fragmentation now has a positive as well as a negative consequence: Smaller planetesimals are lost more rapidly by migration, but are also accreted more readily by cores with atmospheres. Simply put, the two effects largely cancel each other out, and the results of IWI03 are not dissimilar from those of TDL03: For a disk of about ten times the solids and gas density of the minimum-mass model, a $\sim 20 M_{\oplus}$ body forms at 5 AU in $\sim 3 \times 10^6$ years. Unfortunately, even with this improvement, IWI03 finds that very massive disks are required to build Jupiter’s core before the gas disk dissipates, and finds that and it is still not possible to accrete Saturn’s in time.

- Accretion in the shear-dominated regime: In all the work discussed thus far, it was assumed that the velocity dispersion of the planetesimals, v_m , was large enough that the scale height of the planetesimal disk exceeds the radius of the Hill’s sphere, i.e. the disk behaves as if it is fully three dimensional. This occurs if $v_m \gtrsim \Omega r_H$, where Ω is the orbital frequency of the embryo. This situation is referred to as the *dispersion-dominated regime*. However, if gas drag damps planetesimal random velocities strongly enough, v_m can get much smaller than Ωr_H and the system enters the so-called *shear-dominated regime*.

Rafikov (2004; hereafter R04) studied the above situation with an order-of-magnitude analytic analysis. He found that shear-dominated oligarchic growth proceeds in a qualitatively different way, and can be much more rapid, than dispersion-dominated growth (also see Goldreich et al. 2004a,b). The important distinction is that the damping of random velocities is so rapid that between consecutive close encounters with a growing embryo, a planetesimal loses almost all of its eccentricity and

inclination. This makes the planetesimal disk very thin, which increases the accretion rate onto a planetary embryo. In the most extreme case, the velocity dispersion can be so small that the entire vertical column of the planetesimal disk has a scale height less than the protoplanet's Hill radius, thus making accretion a two-dimensional process. In this case, the accretion rate can be much larger than what might be expected in a purely three dimensional situation because planetesimals can no longer pass above or below the embryo. For example, using R04's analytic estimates, at 5 AU the two-dimensional accretion rate is roughly an order of magnitude larger than the oligarchic growth rate with a MMSN and 1 km-sized planetesimals.

At 5 AU, the transition between shear- and dispersion-dominated accretion occurs for planetesimals having sizes of roughly ~ 100 m - 1 km in a minimum mass solar nebula. The transition size increases with distance from the star. In reality, it is likely only a fraction of the total planetesimal population which finds itself in this regime because these objects have a broad size distribution. However, R04 shows that only 1% of the total mass in planetesimals needs to be shear-dominated in order for the accretion rate of embedded protoplanets to be dominated by this part of the population. Indeed, R04 favors an idea similar to that of Wetherill & Stewart (1993), in which planetesimals are in the dispersion-dominated regime, but the small products of their mutual collisions are in the shear-dominated domain and are quickly accreted.

While the work in R04 may supply the long-sought-after solution to giant planet core accretion, Rafikov was forced to make a few significant simplifications in order to perform his analytic analysis. For example, he ignored the role of planetesimal radial migration. Just as a shear-dominated planetesimal receives discrete kicks in random velocity which are then damped, so too will it orbitally decay in discrete jumps, which will tend to remove planetesimals from a protoplanet's feeding zone.

In addition, Rafikov was forced to assume that the surface density of the disk particles will remain spatially smooth. In reality, just as is seen in Saturn’s rings, the planetary embryos will attempt to open gaps in a shear-dominated disk which will significantly lower the accretion rates. R04 suggests that the presence of other embryos might prevent gap opening. However, direct dynamical simulations of problems with similar dynamics have shown that this is not the case (McNeil, Duncan, & Levison 2005; Levison & Morbidelli 2007). In particular, gaps are opened in situations where the embryos are well separated, while the particles become trapped in the L_4 and L_5 Lagrange points if the embryos are closely packed. Thus, the assumption that the disk remains spatially smooth is probably not correct. However, this needs to be studied with realistic numerical experiments in order to determine whether gaps open in the case of giant planets cores, and if they do, how the accretion rate is affected. This is a major goal of this work.

- *The role of collisional damping:* A new scenario for the *in situ* formation of Uranus and Neptune has been proposed by Goldreich et al. (2004a; 2004b, hereafter G04ab). While this new scheme was developed in a gas-free environment, there are elements that could be relevant to solving the core-formation timescale problem. In particular, G04ab envision that during the early stages of oligarchic growth, the growing embryos begin to dynamically excite the planetesimals. As the planetesimal population heats up, collisions between planetesimals become destructive. As a result, the number of planetesimals increase and thus the collisional mean free path decreases. The increased collision rate, in turn, damps the planetesimal’s random velocity. So, independent of the initial sizes of the planetesimals, the system naturally evolves into the shear-dominated regime where accretion rates can be large.

The collisional damping mechanism has a distinct advantage over aerodynamic drag

in that it does not cause radial migration. Thus, it might be possible to preserve Σ_m while keeping v_m small. However, this mechanism still potentially suffers from the gap-opening problem described above (Levison & Morbidelli (2007)). Again, one of the goal of this work is to evaluate the importance of this problem.

- *The role of evaporation/condensation:* Jupiter and Saturn formed in a region of the Solar System where water acts like a solid. Water was so abundant in the solar nebula that the surface density of solids was roughly a factor of 4 larger in regions where water condensed than in areas where it did not. Condensation occurred at the location known as the *snow-line*. We might be able to use the proximity of the giant planets to the snow-line to enhance the solid surface density to even higher levels (Stevenson & Lunine 1988; Cuzzi & Zahnle 2004, hereafter CZ04). From our perspective, the most interesting idea was put forward in CZ04, as we now discuss.

One of the recurring themes in our discussions of core accretion thus far is that the rapid inward migration of planetesimals acts to frustrate planet growth. However, under the right circumstances, CZ04 showed that the opposite can also be true. Indeed, in their model, things actually work *best* if planetesimals are of order meters rather than kilometers in size. The resulting rapid radial migration serves as a means to produce a high local concentration of condensible material, specifically ice. This happens because when ice-rich planetesimals from the outer disk arrive at the snow-line, their complement of water begins to evaporate. CZ04 model the inward flux of ice-rich planetesimals, the water evaporation rate and the diffusion rate of the vapor plume which results, and show that a steady state may not exist until a very large local enhancement in water, between 1 and 2 orders of magnitude, has occurred. Since this vapor plume straddles the snow line, water will recondense onto solid bodies at its outer edge. In this way, the protoplanetary disk receives a large enhancement in

ice over a relatively small radial range ($\Delta a \lesssim 1$ AU). Since accretion rate is $\propto \Sigma_{\text{solid}}$, and isolation mass is $\propto \Sigma_{\text{solid}}^{3/2}$, an increase in the surface density of solids makes it possible to grow bigger bodies faster. Such an enhancement in Σ_{solid} has never been included in a model of core accretion.

The only work of which we are aware that attempted to model most of the above processes in a self consistent way is presented in Chambers (2008). Using a semi-analytic model, Chambers followed the growth of planetary embryos in the giant planet region while they were embedded in a swarm of planetesimals. He included the effects of aerodynamic drag and fragmentation on the planetesimals, and planet-disk tidal interactions (so-called Type I migration; Ward 1986) on the embryos. He found that under a reasonable set of initial conditions, he can produce cores large enough to accrete gas within the disk lifetime.

Although ambitious, Chambers (2008) used semi-analytic methods to follow the evolution of the planetesimals, and thus did not fully account for processes such as gap opening, which has been shown to negatively effect accretion rates in the shear-dominated regime (McNeil, Duncan, & Levison 2005; Levison & Morbidelli 2006). He also did not include the effects of planetesimal driven planet migration (Fernandez & Ip 1984; Hahn & Malhotra 1999; Gomes et al. 2003, Kirsh et al. 2009).

The effects of planetesimal-driven migration have largely been ignored when gas is present because it is believed that Type I migration would dominate. After all, there was a lot more gas than planetesimals in the original solar nebula. The first work of which we are aware that addresses this issue was McNeil, Duncan, & Levison (2005), which concentrated on the terrestrial planet region.¹ They found that, at least for the scenarios

¹Kominami et al. (2005) also put Type I migration and planetesimals in their studies of terrestrial planet formation. However, they artificially increased the capture cross-section

they investigated in this region of the Solar System, planetesimal-driven migration does not counteract Type I migration.

However, there are reasons to believe that the situation may be different in the Jupiter-Saturn zone. For example, the ratio of Σ_{solid} to Σ_{gas} is higher because this region is beyond the snow-line. In addition, the ratio of embryo surface escape velocity to local circular velocity is larger for an embryo at 10 AU than at 1 AU, which might imply that it is a more effective scatterer. Both of these effects would strengthen the effects of planetesimal-driven migration.

To test the above hypothesis we ran the following experiment. We placed a Mars-mass object at 10 AU in a MMSN consisting of both a gaseous disk and planetesimals. The effects of the gas were included by adding fictitious forces to the equations of motion on the solid particles. In particular, we added Type I migration to the planetary embryo using the formalism in Papaloizou & Larwood (2000). Hydrodynamic drag was applied to the planetesimals as if they had a radius of 500 m using the methods in Adachi et al. (1976). In order to save CPU time for this simple experiment, we only placed planetesimals between 8 and 12 AU. The evolution of the embryo’s semi-major axis (a) is shown in Figure 1 — when Type I migration, planetesimal-driven migration, and aerodynamic drag are included, the planet is transported outward! This behavior is due to the fact that the gas density is higher closer to the Sun, and thus aerodynamic drag is stronger and the eccentricity damping timescale is shorter. So, when the embryo scatters planetesimals, those scattered inward are more quickly removed from the planet-crossing region than those scattered outward. In certain circumstances the resultant asymmetry in angular momentum transferred to the planet can overcome tendencies for inward migration found in both gas-free planetesimal

of their objects by a factor of 25 to decrease accretion time. Unfortunately, this will also artificially suppress the relative importance of planetesimal-driven migration.

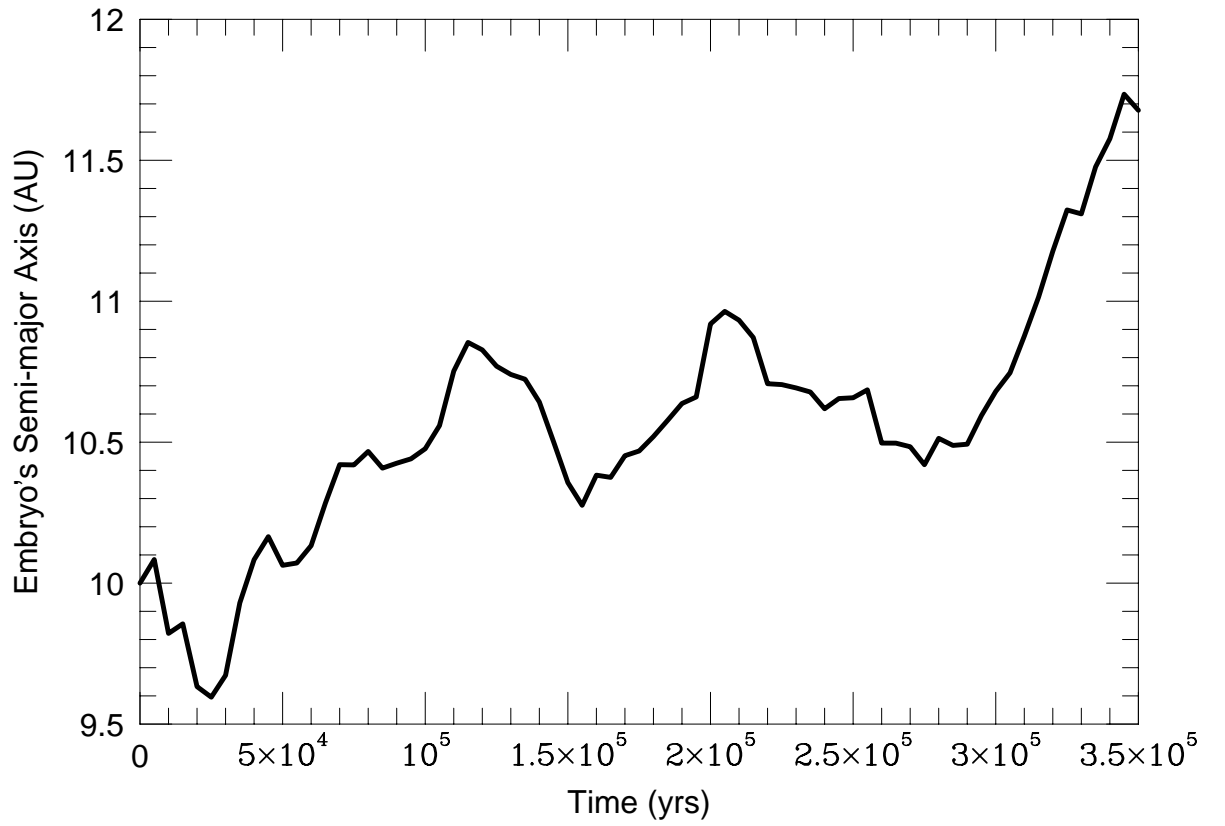


Fig. 1.— The temporal evolution of a Mars-sized object embedded in MMSN disk. We included the effects of Type I migration, planetesimal-driven migration, and aerodynamic drag. Surprisingly, the planet migrates outward.

scattering and Type 1 migration. As a result, the planet migrates outward. Thus, at least in principle, planetesimal-driven migration can overpower Type I migration in the realm of the giant planets. Indeed, we investigate this effect more fully in Capobianco et al. (2009).

So, both the results of the above simple experiment and those of gap opening (McNeil, Duncan, & Levison 2005; Levison & Morbidelli 2006) show that it is important to accurately model the dynamical evolution of the planetesimal swarm in any calculation of core formation. Only full N -body simulations can accomplish this requirement. Such simulations are described in the next section.

3. The Calculations

Our simulations follow the dynamical evolution of a system containing a small number of planetary embryos embedded in a sea of planetesimals. For reasons described at the end of the last section, these are full N -body simulations, where the trajectories of individual objects are followed as they orbit the Sun and interact with each other. Our code is based on SyMBA (Duncan et al. 1998, Levison & Duncan 2000). SyMBA is a symplectic algorithm that has the desirable properties of the sophisticated and highly efficient numerical algorithm known as Wisdom-Holman Map (WHM, Wisdom & Holman 1991) and that, in addition, can handle close encounters (Duncan et al. 1998). This technique is based on a variant of the standard WHM, but it handles close encounters by employing a multiple time step technique introduced by Skeel & Biesiadecki (1994). When bodies are well separated, the algorithm has the speed of the WHM method, and whenever two bodies suffer a mutual encounter, the time step for the relevant bodies is recursively subdivided.

Although SyMBA represented a significant advancement to the state-of-art of

integrating orbits, it suffers from a basic and serious limitation. At each time step of the integration, it is necessary to calculate the mutual gravitational forces between all bodies in the simulation. If there are N bodies, one therefore requires N^2 force calculations per time step, because every object needs to react to the gravitational force of every other body. Thus, even with fast clusters of workstations, we are computationally limited to integrating systems where the total number of bodies is of the order of a few thousand.

Thus, in order to handle the dynamical evolution of a system containing a very large number (roughly 10^{26-29} !) of planetesimals, some compromises needed to be made. We followed the techniques in Levison & Morbidelli (2006, hereafter LM06), where the large number of planetesimals is represented by a smaller number of *tracer particles*. Each tracer is intended to represent a large number of planetesimals on roughly the same orbit as one another. The embryo-embryo and the embryo-tracer interactions are handled directly. However, we made some assumptions in order to calculate the gravitational interaction between the planetesimals. In particular, close encounters between planetesimals are ignored. This is a reasonable assumption because the embryos dominate the viscous stirring of the planetesimals in the oligarchic regime. The overall gravitational potential of the planetesimals is included using a 1-dimensional particle-mesh algorithm described in LM06. This potential must be included in order to correctly handle the resonant interactions between embryos and planetesimals. Indeed, not including it leads to unphysical migration of the embryos, which can be significant when the total mass in planetesimals is comparable or larger than that of the embryos.

In addition to the gravitational interactions, the code described in LM06 also models the growth of the embryos via accretion and the collisional damping of the planetesimals. To accomplish the former, we assume perfect accretion. Recall that we are following the dynamical evolution of the embryos and the tracers using direct N -body techniques. Each

object is assigned a mass and a radius. If two objects collide with one another, we simply merge them while preserving mass, volume, and linear momentum. Note that an important limitation of this code is that only the embryos can grow; the planetesimals cannot.

To incorporate collisional damping between planetesimals we adopt the Monte Carlo techniques described in LM06. In particular, this algorithm performs a particle-in-a-box calculation on a 1-dimensional grid of axisymmetric annuli. In order to calculate the collisional cross-section, the code requires us to specify the radii of the planetesimals. Following standard practice, we assume that all the planetesimals have the same radius, r_p , which is a free parameter in our models.

The LM06 code was modified to include the additional processes described in §2. We now describe each of these in detail.

Fragmentation: The collisional damping algorithm described in the last two paragraphs supplies us with a list of collisions between the planetesimals during our simulations based on Monte Carlo techniques. Included in this information is the impact velocity of the collision, v_{imp} . We use the following Monte Carlo technique to determine whether a particle fragments.

Recall that each tracer particle actually represents a large number (N) of planetesimals of radius r_p . In particular, $N = m_{\text{tr}} / \frac{4}{3}\pi r_p^3 \rho$, where m_{tr} is the total mass associated with the tracer, and ρ is the bulk density, which we assume is 1 gm/cm^3 . In order to keep our calculations tractable, we cannot create new tracers during our simulation. Thus, for each collision, we are forced to simply assume that either none of the planetesimals break, or all of them do. If they break, we assume that the tracer is made up of N_f particles of radius r_f , where $N_f = m_{\text{tr}} / \frac{4}{3}\pi r_f^3 \rho$.

Our algorithm is based on the scaling relationships of Benz & Asphaug (1999,

hereafter BA99), who determined the fragmentation laws for objects composed of a variety of different material. In particular, using hydrodynamic simulations they estimated the ratio of the mass of the largest fragment resulting from a collision, m_{lr} , to the total mass of the colliding pair, m_{tot} . For ice (which we assume), they find that

$$\frac{m_{\text{lr}}}{m_{\text{tot}}} \approx -0.6 \left(\frac{v_{\text{imp}}^2}{2Q_D^*} - 1 \right) + 0.5, \quad (1)$$

where Q_D^* is the critical specific impact energy needed to disrupt the target and eject 50% of its mass. It is also calculated in BA99.

Here we use $m_{\text{lr}}/m_{\text{tot}}$ as a proxy for the probability that a tracer is fragmented. In particular, for each collision we calculate this ratio using Eq. 1. Then we generate a random number between 0 and 1. If the random number is greater than $m_{\text{lr}}/m_{\text{tot}}$, we assume that the tracer particle undergoes fragmentation. Although simplistic, this algorithm has the desired effect because, on average, it produces the correct ratio of fragments to planetesimals in our calculations while preserving the total number of tracers. For example, if we had a collision where $m_{\text{lr}}/m_{\text{tot}} = 0.9$, we would expect to have 10% of the mass in fragments. Our algorithm would disrupt 10% of such collisions and thus, on average, 10% of the mass is also in fragments once we average over a number of collisions.

So, our code contains three types of particles: 1) the embryos which are fully interacting and can grow, 2) a population of tracers representing planetesimals with radius r_p , and 3) a population of tracers representing fragments with radius r_f . In the current version of the code, the fragments do not collisionally damp and they cannot fragment again.

Aerodynamic Drag: The equations of motion of the planetesimals and fragments have been modified to include the effects of aerodynamic drag using the formalism of Adachi et al. (1976). This formalism is accurate for a wide range of Reynolds and Knudsen numbers, and includes as limiting cases what are known as the Epstein and Stokes drag regimes. Our

basic algorithm is described in detail in Brasser et al. (2006). In this case the algorithm has been extended using the prescription of Adachi et al. (1976) to include cases where the Knudsen number is larger than unity, which occurs when a molecule’s mean-free-path is larger than the size of the particle. This can occur for small fragments in the outer region of the nebula.

In order to calculate the drag on particles, we need to adopt a model for the nebula. Our model, which is based on that of Hayashi et al. (1985), has the form

$$\rho_g(\varpi, z) = \rho_{0,g} \left(\frac{\varpi}{1 \text{ AU}} \right)^{-\alpha} e^{-z^2/z_s^2(\varpi)}, \quad (2)$$

where ϖ and z are the cylindrical radius and height, respectively, $\rho_{0,g}$ is the gas density in the plane at 1 AU, and z_s is the scale height of the disk at ϖ . The scale height is determined by the ϖ -dependence of temperature T : following Hayashi et al. (1985) we adopt $T = T_0 (\varpi/1 \text{ AU})^{-1/2}$ so that

$$z_s(\varpi) = z_{0,s} \left(\frac{\varpi}{1 \text{ AU}} \right)^{5/4}, \quad (3)$$

where $z_{0,s}$ is the scale height of the disk at 1 AU. Their “minimum mass ” model has $z_{0,s} = 0.047$, $\alpha = 2.75$, and $\rho_{0,g} = 1.4 \times 10^{-9} \text{ gm/cm}^3$. Theoretical arguments (Lissauer 1987) as well as accretion disk modelling and observational constraints (reviewed by Raymond et al 2007) suggest that the density profile was likely shallower and the overall density at 5 AU higher than suggested by the minimum mass disk model. Thus for the simulations described here, we adopt $z_{0,s} = 0.05$, $\alpha = 2.25$, and $\rho_{0,g} = 3.4 \times 10^{-9} \text{ gm/cm}^3$.

Finally, we need to determine the local circular velocity of the gas, v_g , in our model. As is conventional we define

$$\eta \equiv \frac{1}{2} \left[1 - \left(\frac{v_g}{v_k} \right)^2 \right], \quad (4)$$

where v_k is the local Kepler velocity. For our assumed temperature profile,

$$\eta = 6.0 \times 10^{-4} \left(\alpha + \frac{1}{2} \right) \left(\frac{\varpi}{1 \text{ AU}} \right)^{1/2}. \quad (5)$$

Embryo-Disk Tidal Interactions: For the disk tidal force exerted on an embryo, we use the approach of Papaloizou and Larwood (2000), which the authors developed to handle the case where a protoplanet’s eccentricity can be greater than the scale height-to-semimajor axis ratio. They derive timescales for semimajor axis damping t_a and for eccentricity damping t_e for an embryo of mass M at semimajor axis a with eccentricity e :

$$t_a = \frac{1}{c_a} \sqrt{\frac{a^3}{GM_\odot}} \left(\frac{z_s}{a}\right)^2 \left(\frac{\Sigma_g \pi a^2}{M_\odot}\right)^{-1} \left(\frac{M}{M_\odot}\right)^{-1} \left(\frac{1 + \left(\frac{ea}{1.3z_s}\right)^5}{1 - \left(\frac{ea}{1.1z_s}\right)^4}\right) \quad (6)$$

$$t_e = \frac{1}{c_e} \sqrt{\frac{a^3}{GM_\odot}} \left(\frac{z_s}{a}\right)^4 \left(\frac{\Sigma_g \pi a^2}{M_\odot}\right)^{-1} \left(\frac{M}{M_\odot}\right)^{-1} \left(1 + \frac{1}{4}\left(\frac{ea}{z_s}\right)^3\right) \quad (7)$$

where Σ_g ($= \pi^{1/2} \rho_g z_s$) is the local gas surface density. Papaloizou and Larwood (2000) also argue that if the inclination damping timescale (t_i) is not significantly shorter than the eccentricity damping timescale then it plays little role in the equilibrium state; we set $t_i = t_e$ for simplicity.

From the formulae above we can find the acceleration on an object due to tidal damping of semimajor axis and random velocity, namely

$$\vec{a}_{\text{tidal}} = -\frac{\vec{v}}{t_a} - \frac{2(\vec{v} \cdot \vec{r})}{r^2 t_e} - \frac{2(\vec{v} \cdot \vec{k})\vec{k}}{t_i} \quad (8)$$

where \vec{r} , \vec{v} , and \vec{a} are Cartesian position, velocity, and acceleration vectors, respectively (with r as the magnitude of the radial vector) and \vec{k} is the unit vector in the vertical direction.

We adopt a value of $c_e = 1$, which most researchers agree is reasonable. There is considerably more controversy about the most appropriate value for the coefficient c_a , since it arises from a near-cancellation of torques from either side of the planet and may be strongly affected by nonlinear terms (Paardekooper and Papaloizou 2008). Following the work of many others, we set $c_a = 0$, which implies that we are turning off so called Type I

orbital migration in the simulations presented in this paper. We will consider the effects of non-zero type I orbital migration rates in future publications.

Embryo Atmospheres: As described in §2, the effective capture cross-section of an embryo is significantly increased by the presence of an extended atmosphere that is accreted from the surrounding nebula (II03). In our calculation, we mimic this effect using the formalism developed by Chambers (2006). In particular, assuming the relative velocity of the particles is small compared to the escape velocity of the embryo (which is true in our highly damped simulations) and that the scale height of the atmosphere is set by the energy input due to accreting planetesimals, the effective accretion radius (R_C) of an embryo is

$$R_C^4 = 0.0790 \frac{\mu^4 c R^5 r_H}{\kappa r \dot{m}_R} \left(\frac{M}{M_\odot} \right)^2, \quad (9)$$

where R and r are the radius of the embryo and planetesimal, respectively, M is the embryo’s mass, μ is the mean molecular weight of the atmospheric gas, κ is its opacity, and c is the speed of light. The parameter \dot{m}_R is the accretion rate that the embryo would have had if there was no atmosphere. We calculate this value for each embryo in real time during our simulation by monitoring the number of tracer particles that pass through the embryo’s Hills sphere, and extrapolating to its surface. During our simulations, we did not allow R_C to exceed $0.5 r_H$.

As first described in II03, the existence of an extended atmosphere can significantly enhance the capture cross-section of the embryos. For example, Fig. 2 shows R_C/R for the five embryos in the first simulation presented in the next section during the initial million years of evolution. These embryos are initially $1 M_\oplus$ and grow to an average of $2.1 M_\oplus$ during the time period shown. The increase in R_C/R , however, is due to a decrease in the accretion rate, which occurs because the embryos clear their feeding zone (see discussion below). As can be seen from the figure, R_C can be almost an order of magnitude larger than R in this simulation and the enhancement factor is even larger in some of the other runs.

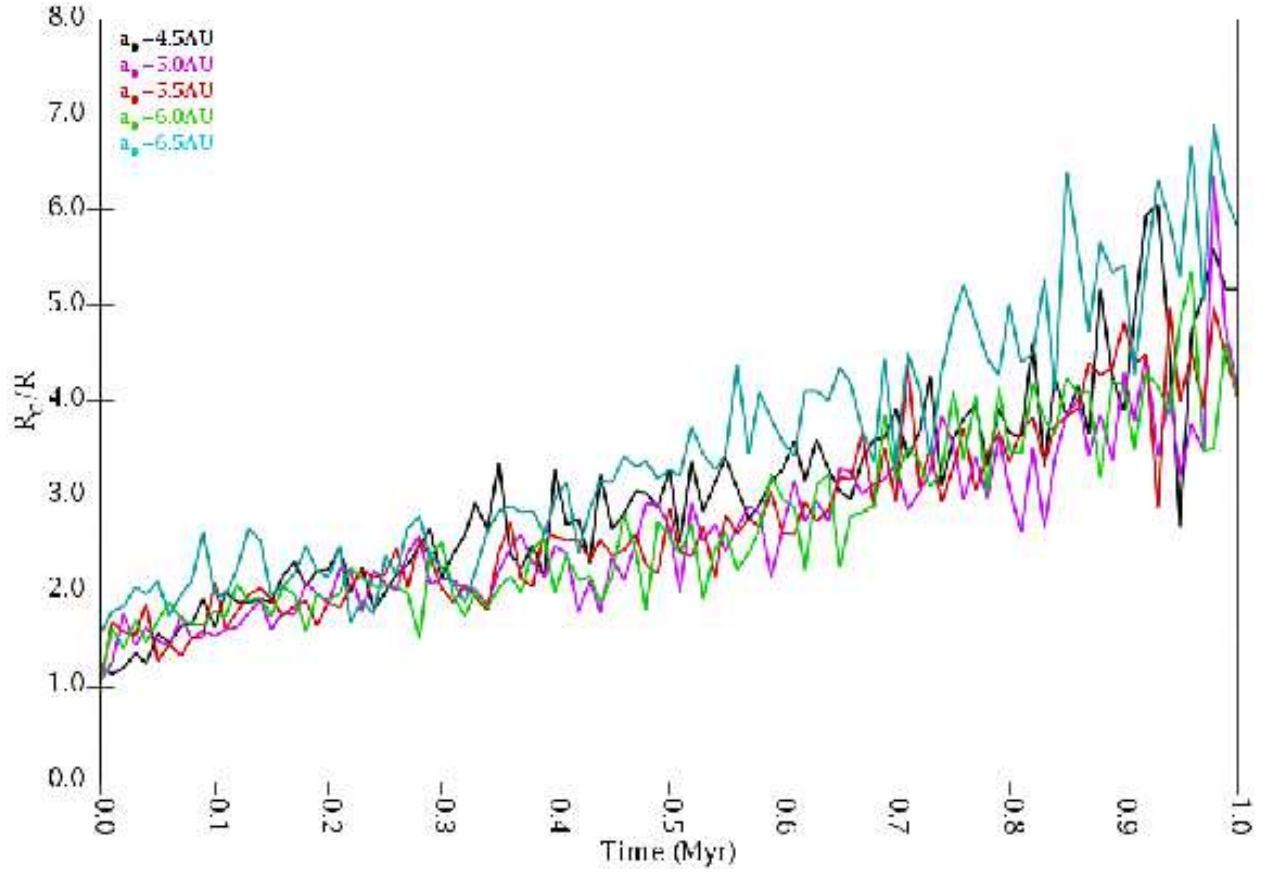


Fig. 2.— The ratio of R_C to R for the 5 embryos in the first simulation discussed in §4. Each embryo is represent by a different color and is identified by its initial semi-major axis, a_0 as shown in the legend.

We next discuss the initial conditions for the majority of our simulations. As described in §1, our goal is not to perform complete simulations of giant planet core formation, but to evaluate the effectiveness of various dynamical mechanisms that might aid in the formation process. As a result, our simulations are somewhat idealized.

We follow the evolution of a system of five Earth-mass embryos embedded in a disk of planetesimals with the code described above. The embryos occupy the region between 4.5 and 6.5 AU so that they are separated by roughly 10 Hill radii. They initially have eccentricities of 0.002 and inclinations of 0.05° . The orientation of their orbits were chosen at random.

These embryos were placed in a planetesimal disk that stretched from 4 to 16 AU. Note that this implies that the embryos were at the inner edge of the disk. We designed our simulations in this way so that the disk is capable of supplying additional planetesimals to the region of embryo growth if physical conditions allow. The disk initially was $200 M_\oplus$, which is six times the minimum mass solar nebula in this region (Hayashi et al. 1985). Previous models (Lissauer 1985; TDL03) have argued that this amount of material is needed to grow the cores. The disk was represented by 20,000 tracer particles. Their eccentricities and inclinations were generated from Raleigh distributions with $e_{\text{RMS}} = 0.01$ and $\sin(i)_{\text{RMS}} = 0.005$. In the next section we describe the dynamical and collisional evolution of this system that occurs as a result of the processes described above. Unless otherwise noted, the simulations were run for 3 Myr, in accordance with estimates for the lifetimes of the gaseous disks (Haisch et al. 2001). However, we held the density of the gas constant during these calculations.

4. Simulation Results

As described in the previous section, our simulations follow the growth of five Earth-mass planetary embryos in the region near Jupiter’s current orbit. Our goal is to determine which combination of effects and parameters will allow these Earth-mass embryos to grow to $\sim 10 M_{\oplus}$ so that they can accrete a massive gaseous atmosphere similar to those of Jupiter and Saturn. Our simulations include a wide range of physical parameters that have yet to be included in any full N -body simulation. The five parameters that we varied are described in detail in §3 and summarized in Table 1. A five dimensional parameter space is too large to cover uniformly. Thus, we probed this space strategically — investigating directions in parameter space that seemed likely to elucidate the roles of the physical processes we are interested in. In all we performed 172 simulations — only a subset of the most illustrative will be discussed below.

r_p :	Radius of planetesimals
r_f :	Radius of fragments
$\rho_{0,g}$:	The mid-plane gas density of the nebula at 1 AU
c_e :	Type I eccentricity decay coefficient
c_a :	Type I orbital decay coefficient
κ :	Opacity of nebular gas

Table 1: A list of the free parameters in our simulations.

We first describe a series of runs intended to investigate the effects of aerodynamic drag on the growth of the embryos. In particular, we studied systems where we turned off fragmentation and varied r_p from 1 to 100 km with a spacing of 0.5 dex. We set $\rho_{0,g} = 3.4 \times 10^{-9} \text{ g/cm}^3$, which produces a solar solid-to-gas ratio for the overall disk. For reasons described above, we set $c_a = 0$, but allowed the gas to damp the eccentricities of the

embryos by setting $c_e = 1$. And finally, we set κ to 2% of the standard interstellar medium value, in accordance with Hubickyj et al. (2005). We performed 15 simulations for each value of r_p . Each of these had slightly different initial conditions. In addition, we changed the seed for the random number generator.

We found that 90% of our simulations exhibited similar behavior. Figure 3 shows the state of such a system ($r_p = 100$ km, hereafter Run A) at 3 Myr. Recall that our goal is to grow the embryos to $\sim 10 M_\oplus$. In this simulation the embryos range in mass from 1.7 to $2.6 M_\oplus$. Note that the region occupied by the embryos has been cleared of planetesimals (except at the embryos’ Lagrange points) and thus we should not expect any more growth. Indeed, all the growth in this simulation occurred in the first million years.

The fact that both the region surrounding the embryos is empty and the embryos only accreted a total of $3.3 M_\oplus$ might seem surprising given that this region originally contained $49 M_\oplus$ of planetesimals. The reason for this can be seen in Figure 3B, which shows the distribution of planetesimals at $t = 0$ (gray histogram) and at $t = 3$ Myr (red histogram). The planetesimals originally between the embryos were scattered away rather than accreted. Aerodynamic drag then removed them from the embryos and placed them on orbits that protects them from encountering the cores. This result shows the importance of including real N -body effects in any study of giant planet core formation. Previous modelling attempts (Hubickyj et al. 2005; Alibert et al. 2005; Chambers 2008), which use semi-analytic approaches to model the embryo-planetesimal interactions, do not allow the embryos to redistribute the planetesimals. Clearly this process is important even when the cross-sections of the embryos are enhanced by an atmosphere.

The dynamical evolution described above did occasionally lead to the construction of $> 10 M_\oplus$ cores. In our simulations we always develop dense, dynamically cold rings of planetesimals immediately exterior to the region containing the embryos (c.f. Fig. 3B). In

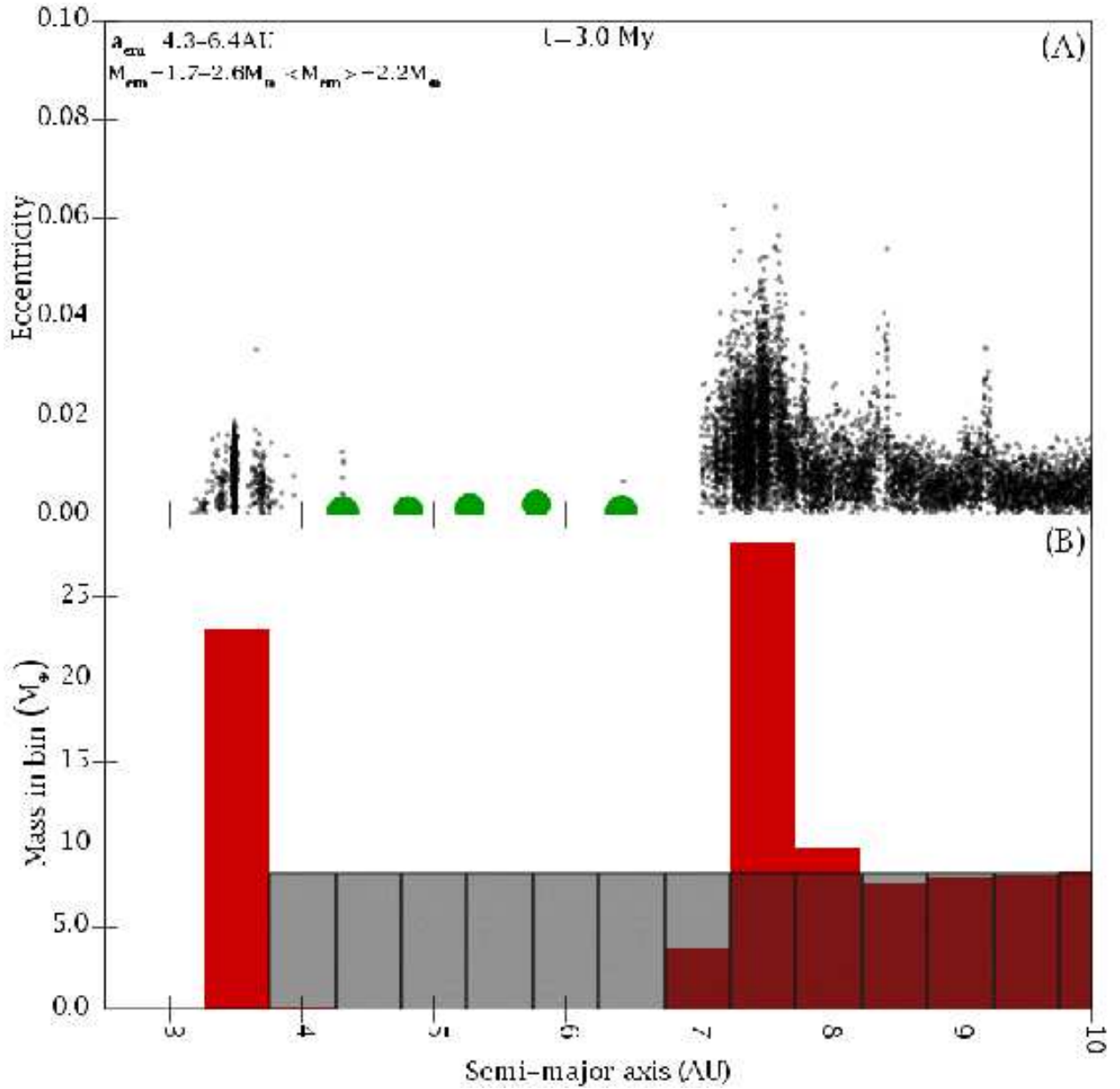


Fig. 3.— The state of the system in Run A at 3 Myr. A) Eccentricity as a function of semi-major axis. The green circles show the embryos, while the black dots are the planetesimals. The size of the green circles are proportional to the cube root of the embryo mass. There are no fragments in this figure (which are normally red) because fragmentation is disabled in this simulation. (B) The distribution of planetesimal mass. In particular, this shows the amount of mass in annular bins that have a width of 0.5 AU. The gray histogram shows the distribution at the beginning of the simulation, while the red shows it at the end.

a few of our simulations the embryos jostle each other enough so the one of the embryos is pushed into one of the rings where it can grow. When this happens the embryo quickly grows $\sim 10 M_{\oplus}$. This primarily occurs in simulations with $r_p = 1$ km.

Unfortunately, we believe that the growth mechanism in the last paragraph probably would not occur in nature, at least to the extent that we observe in our calculations, and is a result of the simplifications that we employ. In the above integrations, rapid growth occurs when an embryo is scattered into a dense, dynamically cold, ring of planetesimals. Such rings form during calculations where damping is large (i.e. r_p is small) in regions that lack the embryos. These rings remain dynamically cold because our algorithm does not allow the planetesimals to dynamically excite one another. In addition, we do not let the planetesimals accrete with one another and thus build another embryo, which would further excite the rings. Since we do not see this rapid growth in runs where the rings do not suffer from a large amount of damping, we think that a more realistic treatment of planetesimal-planetesimal interactions would effectively squelch this mode of growth.

4.1. The Role of Planetesimal Driven Migration

While 90% of the runs in this series followed the behavior where the embryos clear their immediate region and very little growth occurs, the remaining 10% show a new, important mechanism in core formation. This process regularly built $> 10 M_{\oplus}$ embryos and thus is our first success at producing reasonable giant planet cores. In these simulations the embryos undergo a self-sustaining outward migration driven by the gravitational interactions with the planetesimals. This leads to significant growth. An example, which we call Run B, is presented in Fig. 4. This example has the same parameters as Run A, except that $r_p = 10$ km. The embryo that ends up the farthest from the Sun grows from $2 M_{\oplus}$ to $20 M_{\oplus}$ in only $\sim 10^5$ years. Note that our simulations do not include the direct

accretion of nebular gas, and so this $20 M_{\oplus}$ embryo is composed entirely of solids. During the same period, it migrates from 7 to 12 AU.

The system evolves in the following manner. The five embryos are initially in nearly circular orbits and separated by $10 r_H$. They start to grow by eating the nearby planetesimals. Despite the inclusion of dynamical friction with the planetesimals and eccentricity damping due to the gaseous disk, this growth allows the embryos to gravitationally excite one another until they begin to suffer close encounters. At 140,000 years, the inner two embryos merge with one another. In addition at roughly the same time, the second furthest embryo is scattered outward (this appears to be independent of the merger). It then becomes the most distant embryo, but more importantly it penetrated a high density region of the disk. This triggers a period of fast migration and growth. At the end of the simulation (i.e. at 3 Myr), in order of distance from the Sun, the embryos are 6.9 , 3.1 , 5.3 , and $28 M_{\oplus}$.

We performed 15 simulations for each value of r_p . In all the runs that underwent self-sustaining migration, the outer embryo was always the largest and the remaining embryos did not grow to $10 M_{\oplus}$. There is a rough relationship between the mass of the largest embryo in a simulation and r_p . For $r_p = 3, 10, 30$, and 100 km, the average largest embryos were $27, 24, 13$ and $13 M_{\oplus}$, respectively. This is probably due to the fact that there is more damping in systems with smaller r_p and thus accretion is more efficient.

Although not statistically significant, there is also a noticeable trend between the fraction of runs that underwent self-sustaining outward migration and r_p . In particular, four of the simulations with $r_p = 10$ km experienced outward migration, and the number drops off for either larger or smaller radii. This may indicate that outward planetesimal migration could be aided by aerodynamic drag.

In brief, as a planet scatters planetesimals, there are loss mechanisms or sinks both

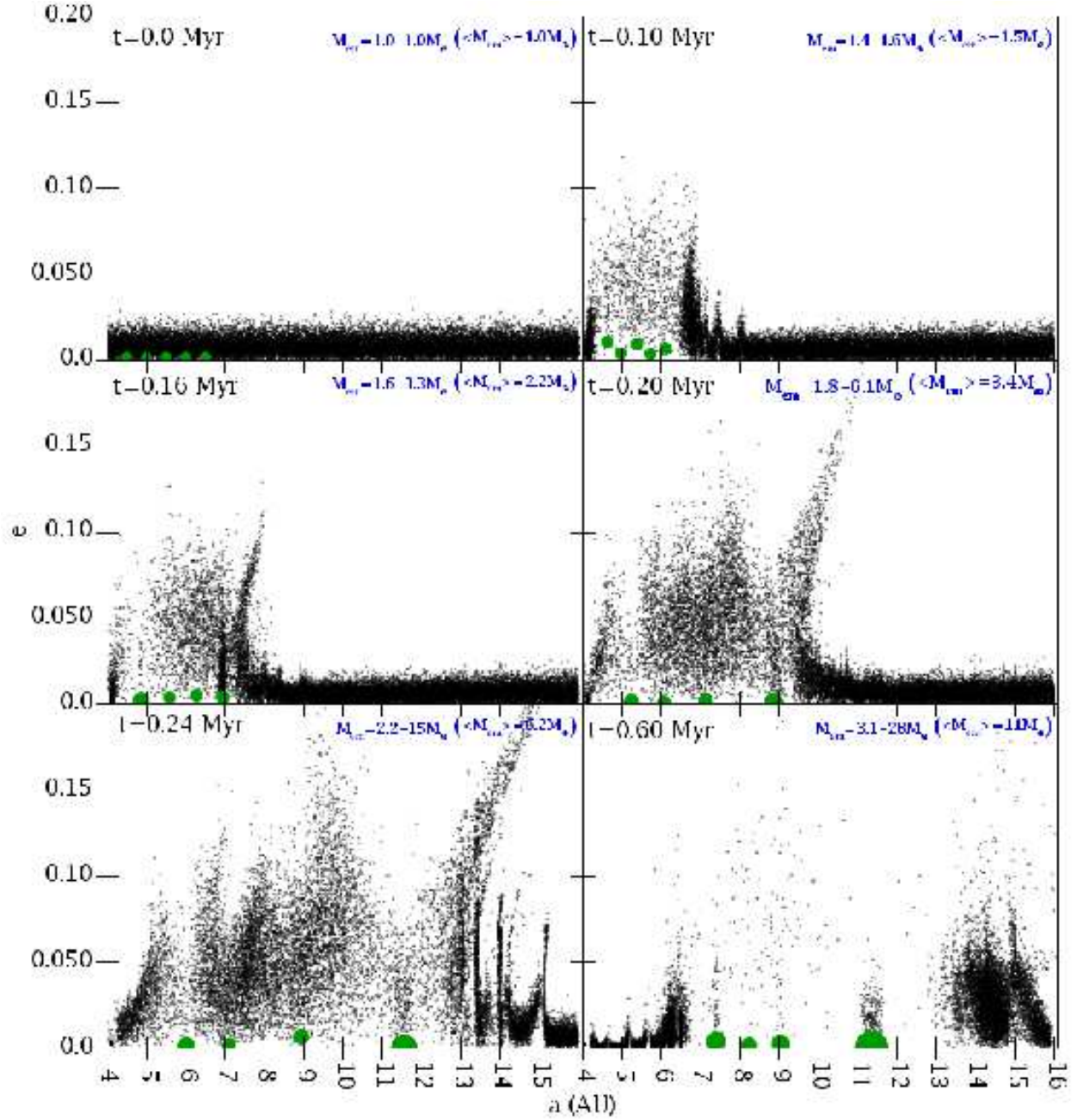


Fig. 4.— The temporal evolution of Run B, which suffers self-sustaining outward migration. See the caption for Fig. 3A for an explanation of these panels.

interior to or exterior to its orbit (see the review by Levison et al. 2007). These sinks can dominate the embryo’s migration and overcome its tendency to migrate inward due to a local asymmetry in outward versus inward scattering (Kirsh et al. 2009). If the interior (exterior) sinks are more important then the embryos will move outward (inward) to conserve angular momentum. At the beginning of migration when an embryo is deciding which direction to go, the only sinks for its planetesimals (in the absence of gas) are passing them off to its brethren, or ejecting them from the system. However, when gas is present, it can be the main factor in determining the direction of migration. Because the density of the gas is a strongly decreasing function of heliocentric distance, an embryo is more likely to lose a planetesimal if it scatters the small object inward where the gas density is highest. That is, the embryo scatters the planetesimals inward, where the gas circularizes the orbit so that it is beyond the reach of the embryo. As a result, there is a major sink interior to the orbit of the embryo that, under the appropriate conditions (combination of $\rho_g(\varpi, z)$ [Eq. 2] and r_p) can trigger outward migration. Important insight into this process can be gained by studying the one-planet case. We do this in Capobianco et al. (2009).

Given the above result, it is interesting to inquire about how much of the growth seen in the outer embryo is the result of its extended atmosphere. Thus, we performed a series of 15 simulations with the same initial conditions as those above (c.f. Fig. 4), but without the atmosphere. We found self-sustaining outward migration in only one of these simulations. While 1 out of 15 is not necessarily statistically distinct from the 4 out of 15 found above, the character of the migration is different. Like the run shown in Fig. 4, there was a burst of migration that pushed the outermost embryo from 7 to beyond 11 AU in only 60,000 years. The major difference between this and previous runs is that during the migration the embryo grew by only $0.6 M_{\oplus}$. Indeed, by the end of the simulation the largest embryo was only $3.5 M_{\oplus}$. Thus, we tentatively conclude that a massive gaseous envelope greatly increases the probability of substantial growth of the embryos during planetesimal driven

migration.

Given the success of our simulations that combine massive atmospheres and planetesimal driven migration, we must address the fact that only $\sim 10\%$ of our simulations underwent outward migration before we can conclude that this mechanism is a viable solution to the core formation problem. We believe, however, that this process might be more robust than the above models suggest. For reasons described previously, the above simulations contain many simplifications. Perhaps most important for this issue is that both the embryos and the planetesimals are represented by objects of a single size. We can imagine that, for example, if the planetesimals were represented by a more realistic size-distribution, there might routinely be enough objects at the correct size to cause this outward migration. Unfortunately, our code cannot handle this situation (see however, Capobianco et al. 2009), but it can currently accommodate embryos of different initial masses. Thus, we performed a series of simulations with the same parameters as the Run A and with r_p was either 1, 10, or 100 km. In addition to the 5 Earth-mass embryos, however, we added a population of 10 additional $0.1 M_\oplus$ (i.e. \sim Mars-mass) embryos. The initial conditions for these simulations are shown in Fig. 5A.

Before we describe the results of these calculations, we first must issue a warning. As described above, in these calculations we use a population of 20,000 tracer particles to act in place of a much larger number of planetesimals. Previous studies (e.g. Levison & Morbidelli 2007) have shown that this representation is valid as long as the embryo to tracer mass ratio is $\gtrsim 100$. This is true for our main simulations where the mass ratio is precisely this value. Indeed, it is for this reason that we restricted our main studies to Earth-mass embryos in the first place. However, in the experiments we are about to discuss, the ratio is only 10. Thus, the \sim Mars-mass embryos are experiencing significantly larger Brownian motion than a more realistic simulation would produce. (Unfortunately, it is

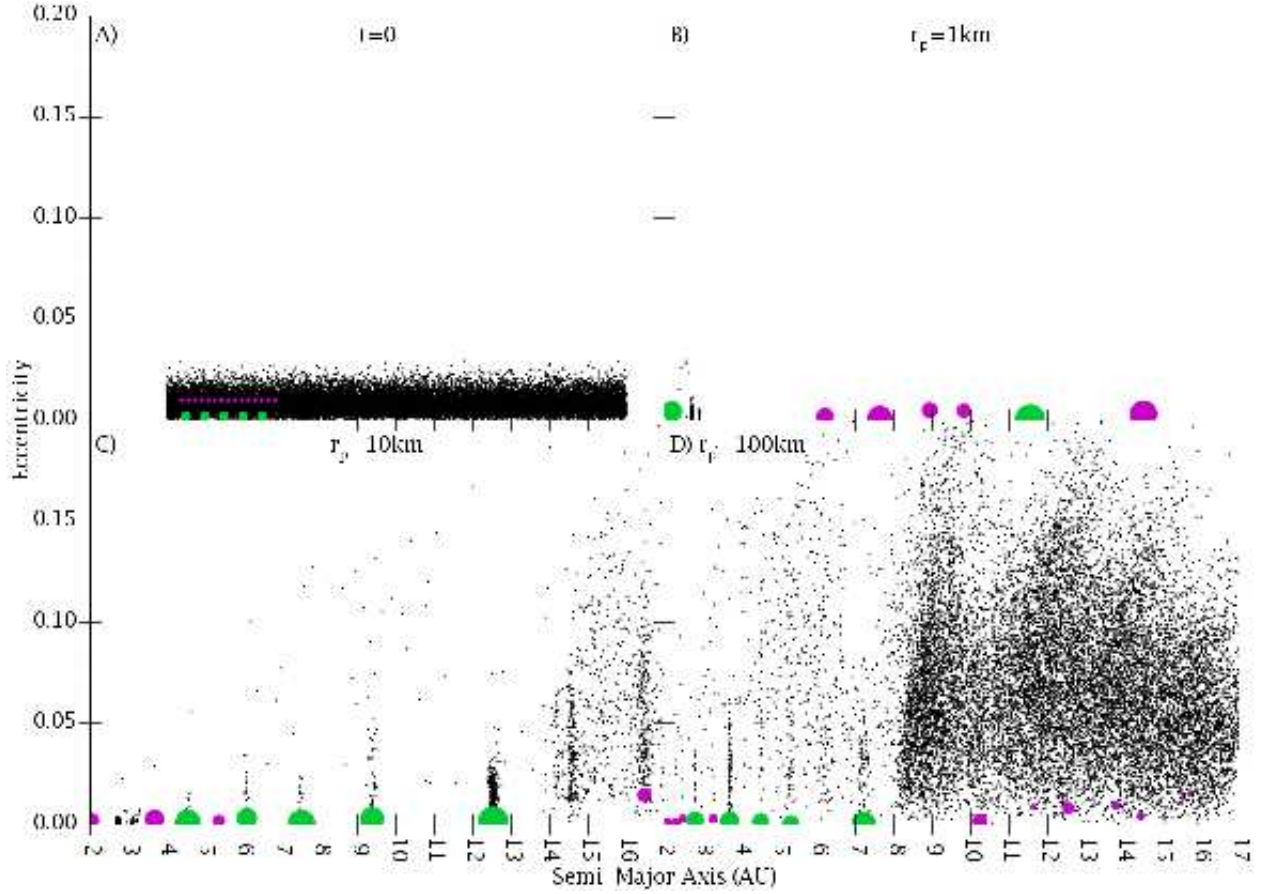


Fig. 5.— A) The initial conditions for the simulations that contain \sim Mars-mass embryos. See Figure 3 for a description of the colors and symbols. Here, the green represents the initial Earth-mass embryos, while the purple shows the initial \sim Mars-mass embryos. B) $r_p = 1$ km at 3 Myr. C) $r_p = 10$ km at 3 Myr. D) $r_p = 100$ km at 3 Myr.

not practically feasible to significantly increase the number of tracers.) Thus, the results of these simulations should be viewed with caution. Have said this, we believe that these simulations show that self-sustaining outward migration might be significantly more robust than the simple simulations discussed above would imply, and thus we briefly discuss them.

Figs. 5B–D show each system at 3 Myr. In both the $r_p = 1$ and 10 km calculations self-sustaining outward migration is clearly apparent because there are objects that were originally Earth-mass embryos (green in the figure) at 11.6 and 12.5 AU, respectively. Outward migration also occurred in the $r_p = 100$ km simulation, but the embryos migrated back in. Indeed, the embryo started at 6.5 AU, migrated to 10.5 AU in 10^5 yr, migrated back to 6.1 AU, out to 8.5 AU, back to 6.0 AU, and at the end of the simulation is migrating outward again. Therefore, rather than being a rare occurrence, outward migration is the norm in these simulations.

The big embryos migrate because of the effects of their smaller relatives on the planetesimals. In all cases we see that, although the \sim Mars-mass embryos were initially distributed among their larger brethren, a significant fraction are scattered out of this region on the timescale of a few $\times 10^4$ years. Most of these evolve onto nearly-circular orbits just outside of it. Recall that in Run A (Fig. 3) many of the planetesimals scattered from between the embryos are also trapped in this region. It is not surprising that the \sim Mars-mass embryos behave like the planetesimals when they interact with the Earth-mass embryos because in both cases the mass ratio is large.

It is important to note that in these runs, the \sim Mars-mass embryos that come to populate the region beyond the Earth-mass objects actually feed planetesimals back inward. This process causes some of Earth-mass embryos to migrate outward. The smaller embryos are pushed outward as well. Thus, the whole system spreads and the embryos grow, resulting in the systems seen in Figs. 5B–D. In each of these three simulations, objects

originally $1 M_{\oplus}$ grew to $> 10 M_{\oplus}$ — the largest being $28 M_{\oplus}$. Indeed, four of the five big embryos in the $r_p = 10$ km run grew larger than $> 10 M_{\oplus}$, and the fifth was $8.7 M_{\oplus}$.

The issue now is how to interpret the success of these simulations given the above warning. The main difference between these runs and the ones with five embryos is that the large cores deliver the \sim Mars-mass objects to a region where they can feed planetesimals back inward. We see no reason why the low-resolution of the disk should effect this evolution. Thus, we feel that this part of the simulations would indeed happen in a more realistic model.

We believe that these calculations show that self-sustaining outward migration would commonly result if we could include a spectrum of embryo sizes. Indeed, systems with a strong size gradient are a probable outcome of the earlier phases of planet formation: analytic models of oligarchic growth (Thommes et al. 2003) predict that prior to growing to their isolation masses, the embryo masses should vary as a^{-X} , with $X \sim 6$ for the surface density distribution we use here. Thus one expects that at the time that an oligarchic embryo approaches a mass of $\sim 1 M_{\oplus}$ near 5 AU, embryos beyond 7.5 AU will each be more than an order of magnitude smaller in mass. Again, we use similar size embryos between 4.5 and 6.5 AU in our main simulations in order to adequately resolve the the embryo-disk interactions. It still remains to be demonstrated whether a more realistic size spectrum will actually lead to $10 M_{\oplus}$ cores. Unfortunately, we must leave this work to the future.

4.2. The Role of Fragmentation

As described in §2, it is believed that fragmentation will aid core formation because the small remnants of a planetesimal-planetesimal collision will damp quickly and thus be more likely to be accreted by the growing embryos (Wetherill and Stewart 1993; R04). One

of the main motivations of this work is to test this hypothesis.

Fig. 6 shows the evolution of a system with the same characteristics as Run A under the influence of fragmentation with $r_f = 100$ m. Early on, the system behaves as one would expect. The embryos dynamically excite the planetesimals (black dots in the figure). This leads to collisions which fragment the planetesimals. Due to their much smaller size, the fragments (red dots) have much smaller eccentricities than the planetesimals (the RMS eccentricity is 0.006 as opposed to 0.03 at $t = 40,000$ yr). Also, they spiral inward at a much faster rate. For the aerodynamic drag models described in §3, Adachi et al. (1976) show that gas drag will cause a fragment with physical density ρ_f , eccentricity e and inclination i to decay in semimajor axis a at a rate given for small e and i by

$$\frac{da}{dt} = -\frac{2a\eta}{\tau_0} (0.97e + 0.64i + \eta), \quad (10)$$

where η , which is defined in Eq. 4, is a function of the ratio between the circular velocity of the gas and the local Kepler velocity, and

$$\tau_0 = \frac{8\rho_f r_f}{3C_D \rho_g v_k}. \quad (11)$$

Thus, near 5 AU in the nebular model we have adopted, 100 m fragments on near-circular orbits ($e, i \ll \eta$) would be expected to migrate inward at roughly 2×10^{-5} AU/yr. However, rather than sweeping by or being accreted by the embryos, the fragments typically become trapped in mean motion resonances. For example, the clump of fragments near 5.2 AU in the $t = 500,000$ yr panel is in the 11:10 mean motion resonance with outer embryo. This clump contains a total mass of $1.3 M_\oplus$.

Once in resonances, the embryos try to stop the inward migration of the fragments (Weidenschilling & Davis 1985). However, the gas continues to draw angular momentum from the fragments' orbits. The interaction between the resonance and the aerodynamic drag pumps up the eccentricities of the resonant particles in the clump (to values of

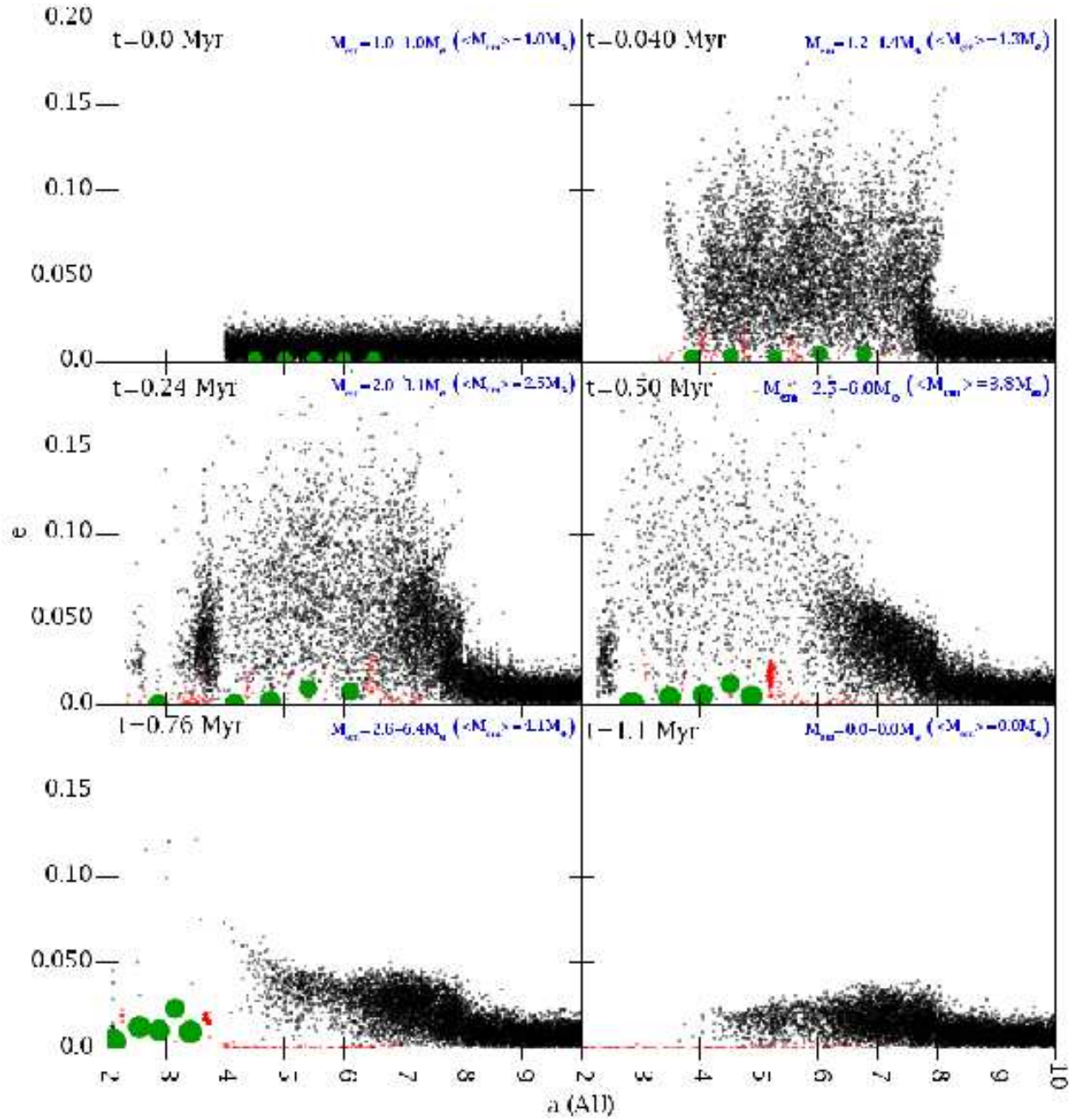


Fig. 6.— The temporal evolution of a system like Run A, but in which fragmentation is turned on. See the caption for Fig. 3A for an explanation of these panels. Note that the red dots represent fragments of collisions.

~ 0.015 , consistent with the prediction of $[\eta/(j+1)]^{1/2}$ for a $j/(j+1)$ resonance by Weidenschilling and Davis 1985). The larger eccentricity increases the rate at which the fragments attempt to spiral in to $\sim 10^{-4}$ AU/yr (cf. Eq. 10). However, the resonance lock means that the angular momentum loss is shared with the interior planet, and by virtue of that body’s interactions with the planets interior to it, with the whole retinue of planets. Thus, although the drag acts directly on the $1.3 M_{\oplus}$ of fragments, the whole ensemble of $\sim 22 M_{\oplus}$ ”shares” the angular momentum loss and the group migrates in at roughly 1/20 of the rate predicted for fragments of that eccentricity. Consequently, by 1 million years, the embryos are pushed inside of 2 AU.²

A note of caution is now in order. As we described above, we do not allow fragments to collisionally interact with one another in these calculations. The embryo migration rate is determined, in part, by the eccentricities of the fragments. This, in turn, is dependant on the eccentricity damping rate, which is, in reality, affected by both aerodynamic drag and collisions. By not including fragment collisional damping, we are overestimating the eccentricity and thus the embryo migration rate. In addition, there is the potential that a collision between two resonant objects could knock them out of the resonance. In order to estimate these effects, we have performed simulations of a system containing one embryo and a series of particles in the embryo’s 7:6 mean motion resonance (which is commonly populated in our main simulations). We find that collisions were very inefficient at removing objects from the resonance. Indeed, the libration amplitudes of the particles decreased during the simulation. The migration rate of the embryo in the calculation without collisions is only 1.6 times larger than that with collisions. Thus, although the

²The timestep of our calculations is determined by the shortest orbital period in the problem. Thus, in order to keep the timestep large enough to make the calculations practical, we removed any object that got closer to the Sun than 2 AU.

effect of collisions is significant in the quantitative sense, we believe that the fact that it was not included does not invalidate our basic conclusion that resonant trapping can lead to wholesale inward migration of the growing cores.

Earlier work (Weidenschilling & Davis 1985; Kary et al. 1993) also tells us that not all small objects undergoing radial drift due to aerodynamic drag will be caught in resonances. The probability of capture is determined, in part, by the strength of the drag acceleration. So, our conclusion above might not be robust in that there might be large regions of parameter space in which resonant trapping does not occur. To test this, we performed a series of simulations where we varied r_f from 1 to 100 meters with a resolution of ~ 0.5 dex. We performed integrations with r_p set to both 10 and 100 km — the former chosen in the hope that planetesimal driven outward migration could negate the effects of resonant trapping. We found that for $r_f \geq 30$ m all the embryos were lost by being pushed inward by the fragments.

The runs with $r_f \leq 10$ m behaved as the analytic and numerical experiments models cited in the last paragraph found. That is, fragments were created in planetesimal collisions, were damped by the gas, spiraled inward, and were accreted by the embryos while in very low-inclinations orbits (i.e. in the shear regime) or migrated right past, as happened most often for the smallest fragments. No resonant trapping was observed because the fragments were migrating faster than the critical value at which trapping begins to be ineffective (Kary et al. 1993).

We find that this process only allows for a significant amount of growth for a narrow range of r_f — in particular when $r_f = 10$ m for the gas disk adopted here. In order to understand this, we must first discuss the case where the embryos grew substantially. Fig. 7 shows a simulation where all 5 embryos reach a mass of nearly $10 M_\oplus$ (the inner one is actually $\sim 9.5 M_\oplus$, but the rest were $> 10 M_\oplus$). In this run, which we call Run C, all the

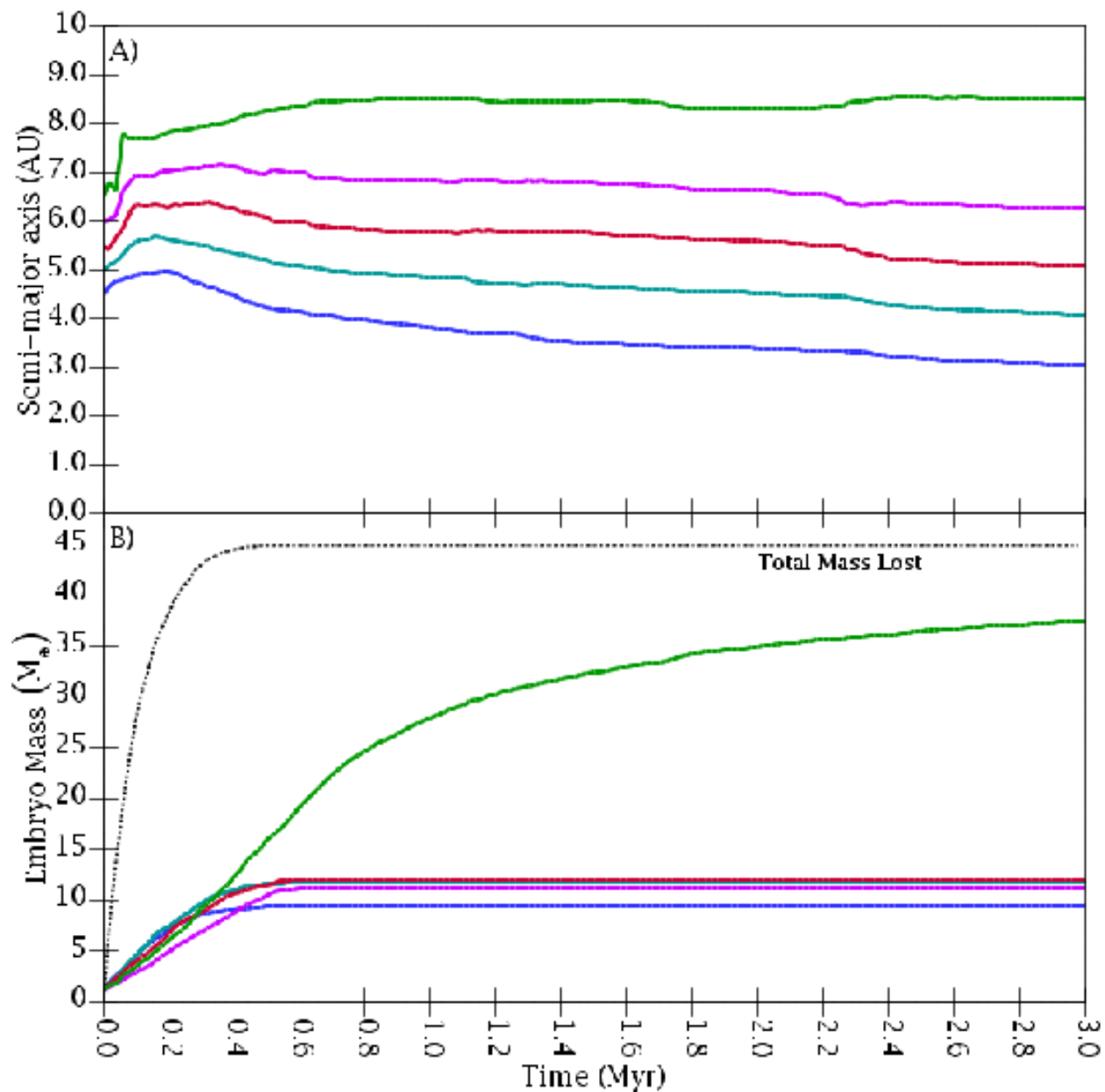


Fig. 7.— The temporal evolution of the five embryos in the run with $r_f = 10$ m, $r_p = 10$ km, and κ to 2% of the standard interstellar medium value. A) The semi-major axes as a function of time. Each embryo is represented by a solid curve of a different color. B) The mass as a function of time. The solid curves show the embryos, where the color corresponds to the semi-major axes in (A). The dotted curve show the mass lost from the system because it got too close to the Sun.

embryos enjoy a roughly linear growth in mass for the first $\sim 400,000$ years. After this time, growth of all but the outermost embryo stops. The outer core continues to grow until it is $38 M_{\oplus}$ at the end of the simulation.

The dichotomy between the outer embryo and the rest of the oligarchs supplies an important insight into how the accretion efficiency varies in these simulations. Clearly, near the end of the simulation, the outer embryo gets large enough that fragments generated in the outer disk (recall that the outer embryo moves between 6.5 and 8.5 AU, while the disk extends to 16 AU) cannot escape as they sweep by. Thus, it grows, while its neighbors starve. This situation was not always the case. Fig. 8 shows the fate of fragments that were created beyond the orbits of the growing cores as a function of the outer embryo mass. In particular, the ordinate indicates the fate of a fragment, which can be either accretion by Embryo N , where N ranges from 1 to 5 in order of increasing heliocentric distance, or getting too close to the Sun (marked as ‘Lost’). The abscissa is the mass of the outer embryo. Note that at early times (i.e. before 400,000 years) this can be used as a proxy for the mass of all the embryos since they were roughly the same at these times (Fig. 7B). The color in the figure shows the probability that a fragment that formed far from the Sun will reach one of the fates listed.

When the cores were $\sim 1 M_{\oplus}$, the probability that an embryo will capture a fragment as it sweeps by is small and thus the embryos grow at an equal rate. Note that at this time, half of these fragments were removed from the simulation because they got too close to the Sun, implying that a particle only had a 13% chance of being accreted by any individual embryo. This efficiency is similar to that found by Kary et al. (1993) for a core with relatively small envelope. By the time the embryos reach $10 M_{\oplus}$, the probability that a particle will survive the passage of an individual embryo is roughly 40% — reaching 90% at a mass of $18 M_{\oplus}$. This higher efficiency is due to the fact that an extended gas envelope

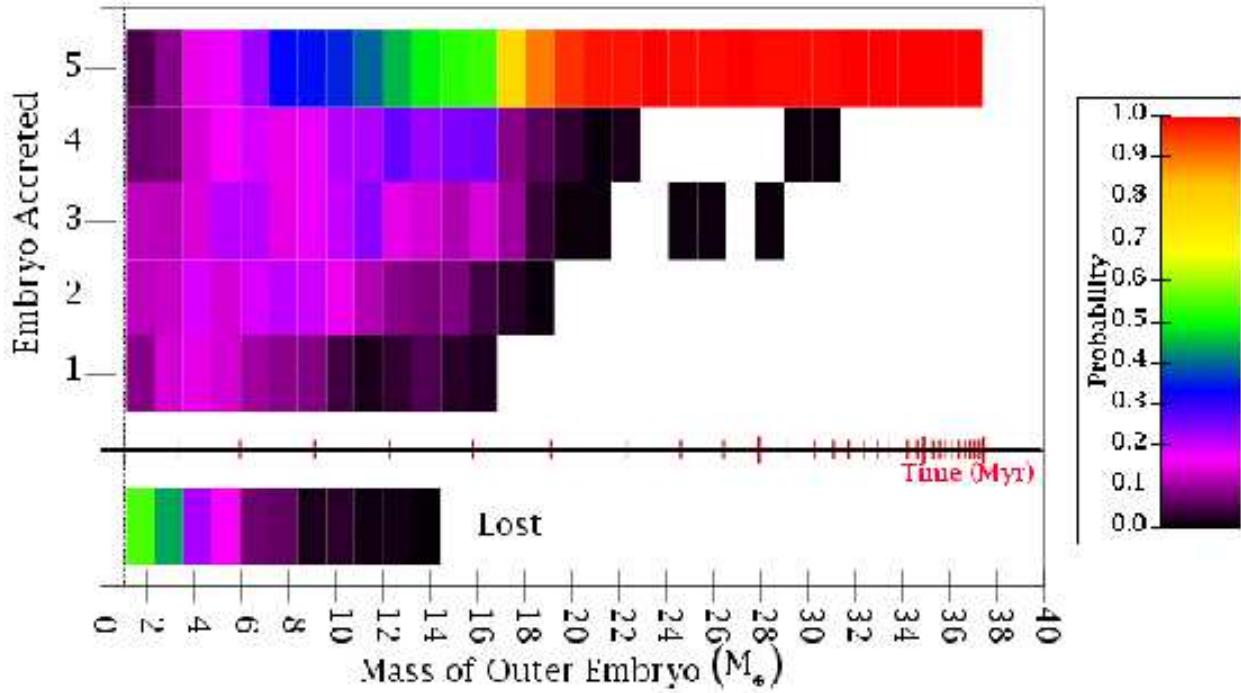


Fig. 8.— The probability that a fragment created beyond the orbits of the embryos will suffer a particular fate as a function of the mass of the outermost embryo. In this figure, the color represents the probability of the fate given on the ordinate. A fragment can either be accreted by an embryo (which are numbered as a function of increasing heliocentric distance), or get too close to the Sun (indicated by 'Lost'). The red tickmarks indicate time, where the small and large marks show a spacing of 10^5 , and 10^6 years, respectively.

has caused the effective radius of capture of fragments to be a fairly large fraction of the embryo’s Hill sphere. It is important to note that our simulations do not include run-away gas accretion or allow the embryos to open a gap in the gas disk. Thus, these simulations are not applicable for masses larger than $\sim 10 M_{\oplus}$.

Given the above discussion, it might be tempting to conclude that most of the mass accreted by the inner four embryos came from the distant disk. However, this is not the case. Fig. 9 shows characteristics of the particles that were accreted by the Embryo 3 during the simulation. The abscissa in Fig. 9A is the semi-major axes of a particle at the beginning of the simulation and the ordinate is the time that the particles were accreted. The color is the total mass from that particular semi-major axes that was accreted at that particular time. Fig. 9B is similar, but instead of showing the initial semi-major axes, we plot the semi-major when the particle became a fragment because of a collision.

We interpret this figure as follows. In Fig. 9A, the accretion occurred during early times (which we already know from Fig. 7). In addition, the whole region between 4 and 8 AU is yellow, indicating that the core mainly feeds on objects that were basically uniformly spread between the embryos. However, Fig. 9B shows that most of these particles accreted by this embryo suffered catastrophic collisions near ~ 9 AU. This is due to the fact that, although the objects eaten by Embryo 3 formed in amongst the embryos, they were initially scattered outward forming a dense ring of material outside of the orbits of the embryos. This is similar to what happened in Run A (c.f. Fig. 3). Once in this ring the planetsimals fragmented and spiraled inward due their increased drag, only to impact an embryo. Once the outer embryo became large enough to capture all of the fragments, Embryo 3 stopped growing. Indeed, objects that were accreted by the outermost embryo show a similar behavior (see Fig. 10) in that they were scattered into the ring before they fragmented. However, this embryo continued to feed for the length of the simulation

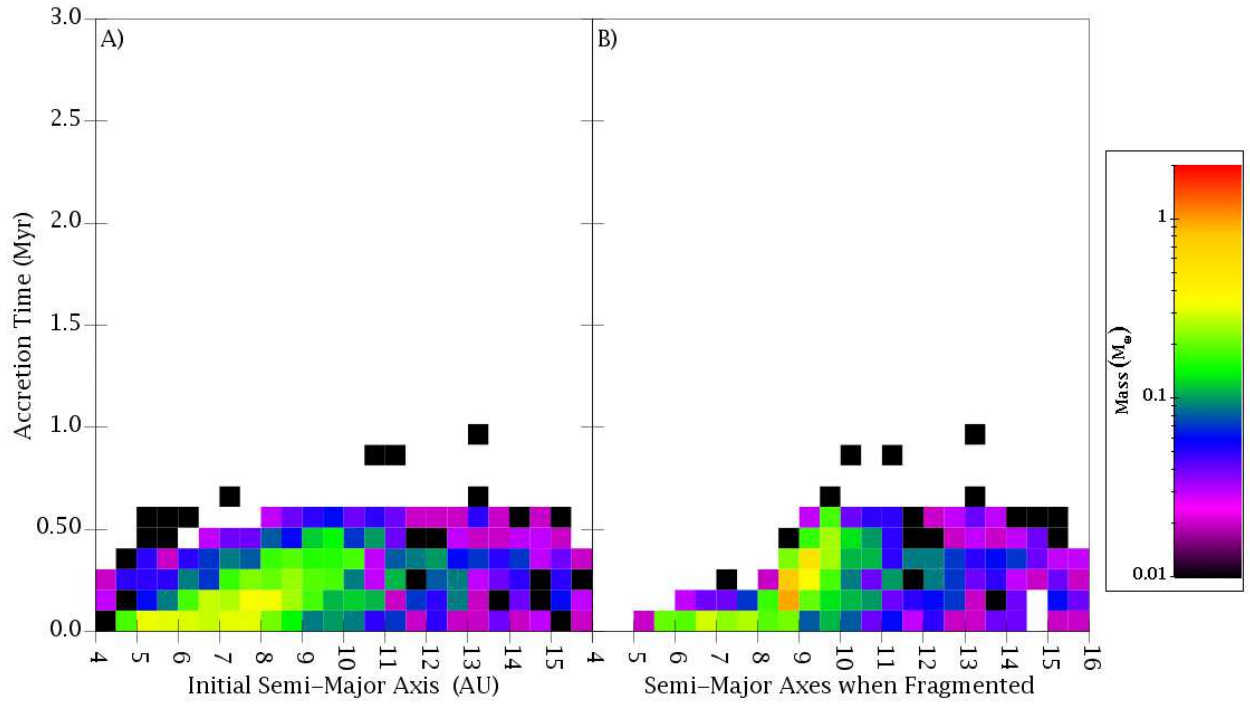


Fig. 9.— An analysis of objects eaten by the Embryo 3 of the simulation shown in Fig. 7. In particular, the color shows the amount of mass accreted as a function of location (on the abscissa) and the time that the object was accreted (ordinate). A) The initial semi-major axis of the planetesimal. B) The Semi-major axes where the planetesimal fragmented.

because of its favorable location.

With the insight gleaned from the above discussion, we can now use Fig. 8 to grasp why we only get significant growth when $r_f = 10$ m. As described above, this figure shows that at the beginning of the simulation, the capture efficiency of the embryos is about 13%. While this is small, it is large enough to allow the embryos to begin to grow. This is illustrated in a run we performed that is similar to Run C, but with $r_f = 3$ m. For this simulation, the capture efficiency was only 2.7% (again consistent with the results of Kary et al. for such rapidly migrating fragments) and thus although $95 M_\oplus$ of fragments went through the region populated by the embryos, the embryos grow to only $\sim 3.6 M_\oplus$. For the same $95 M_\oplus$ of fragments, an accretion probability of 13% predicts that the embryos should grow to $12 M_\oplus$ each. Thus, the capture efficiency is simply too small for $r_f < 10$ m. And since the fragments force the embryos too close to the Sun for $r_f > 10$ m, we must conclude that significant growth only occurs for a narrow range of aerodynamic drag parameters.

The other issue along these lines that must be discussed is the role of the embryo atmospheres. Here, luckily we have some good news. We performed a series of runs similar to Run C, but where we varied the opacity of the atmosphere, κ , from 0.002 to 100 times the interstellar value. We find that significant growth in all the simulations, although the resulting embryos were slightly less massive in the simulations where κ was larger (i.e. the effective radius of the embryos were smaller, see Eq. 9). Note, however, that the embryos only grew to $\sim 3 M_\oplus$ in the simulation with no atmosphere at all. These results demonstrate that although an atmosphere is required for significant growth, its usefulness is not particularly sensitive to opacity.

Earlier in this subsection we mentioned that we performed simulations with $r_p = 10$ km in the hope that planetesimal driven outward migration would counteract the tendency for the fragments to push the embryos inward. To test this hypothesis, we performed

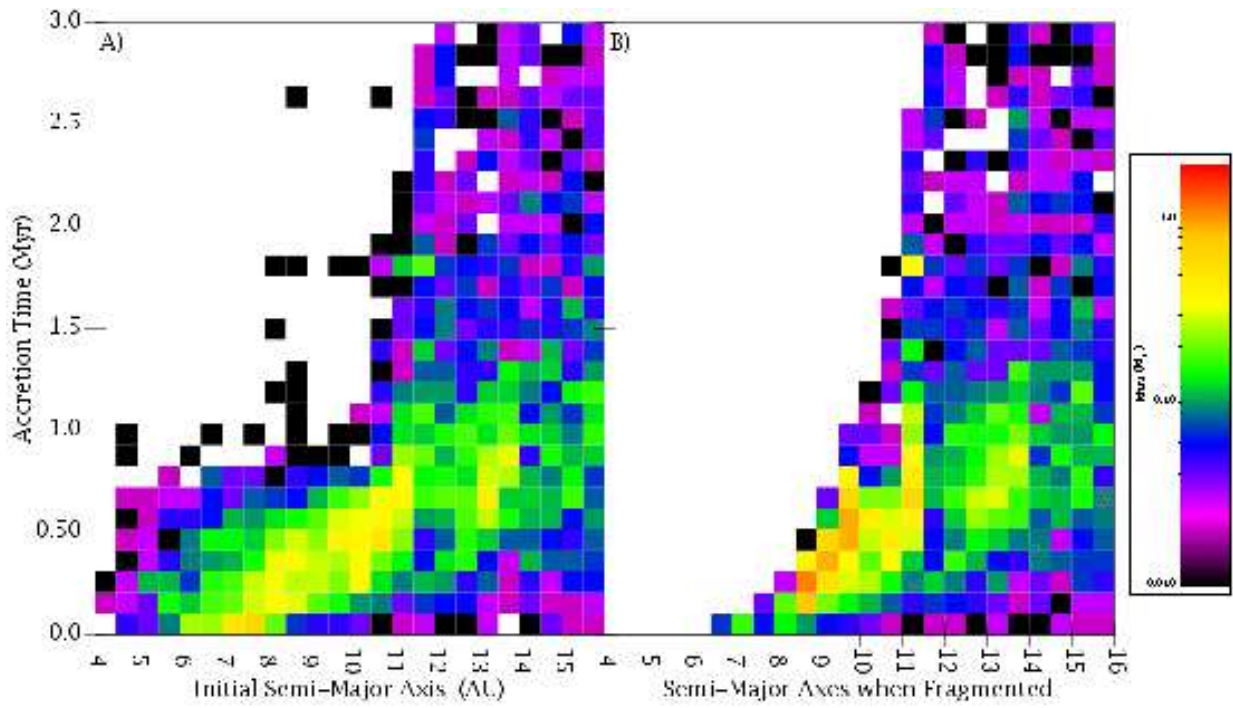


Fig. 10.— Same as Fig. 9, but for the outermost embryo.

seven simulations like Run C, but with $r_p = 10$ km and $r_f = 10$ m. The only difference between the runs is that we used a different random number seed and moved the outer embryo by roughly 10^{-5} AU. In all cases, the embryos were pushed inward and out of our simulation. Thus, we tentatively conclude that planetesimal driven outward migration is not an important process in situations where push-in occurs.

Note that the embryos do migrate outward in simulations that have fragmentation if r_f is small enough that resonant trapping does not occur. However, they do not grow as massive in these simulations as they did when fragmentation was turned off. In a simulations with $r_p = 10$ km and $r_f = 1$ m, the outer embryo only grew to $13 M_\oplus$. Note that this is still large enough to be considered a legitimate giant planet core. The only way we see to save planetesimals driven migration as a viable mechanism for core accretion is if either: 1) the planetesimals are strong so that they do not break, 2) they are pulverized during collisions so that all the fragments are smaller than ~ 10 m, or 3) they undergo a collisional cascade fast enough that they are not dynamically important when they are ~ 100 m in size.

We now return to the issue of whether fragmentation can be a general aid to growth and ask if there is a way to circumvent the problem that substantial growth only apparently occurs for a narrow range of aerodynamic drag parameters. One possibility is to once again invoke our \sim Mars-mass embryos. It is possible to imagine a situation where these smaller embryos gravitationally scatter fragments out of resonances, thereby stopping their inward push on the embryos and allowing the fragments to be accreted. This turns out not to be the case. We performed three simulations similar to the ones shown in Fig. 5, but where we turned on fragmentation with $r_f = 10$ m. Unfortunately, in all the cases, the original Earth-mass embryos were pushed out of the simulated region by the fragments.

What other alternatives are there? As described several places above, once a tracer

becomes a fragment of a particular r_f , we did not allow it to collisionally evolve any further. Although, we argue above that collisions will not significantly alter the dynamics of the resonant particles, it is possible that collisions will fragment the objects further so that they will be able to leave the resonance due to aerodynamic drag. This may be important given that the collisional optical depth can be much larger than one. We can only speculate as to how the fragmentation of our fragments will affect the above results. Some insight is available in the literature. We find that the typical impact velocity between objects in the resonances is roughly 100 m/s. For objects of, say, 100 m the critical speed for catastrophic disruption is only 3 m/s (Stewart & Leinhardt 2009). These collisions are so energetic that the resulting fragments are probably so small (Stewart-Mukhopadhyay, pres. comm.) that they would sweep by the planets without getting accreted.

More generally, our results reveal that accretion is only efficient for a narrow range of planetesimal sizes, and, although we model the collisional cascade crudely, we see no reason why this result should not extend to more realistic situations. Both observations of asteroid families (see Zappalà et al. 2002 for a review) and analytic and numerical models (BA99; Durda et al. 2007) show that collisionally processed populations exhibit a size distribution that approximately follows a power-law. Thus, we believe that if we could model the collisional evolution of our system more accurately, we would find that only a small fraction of the small bodies would be found in the ‘sweet-spot’ for accretion. As a result, we believe that fragmentation is not the general solution to the core-formation problem.

4.3. The Role of Evaporation and Condensation

As we described in §2, the problem of core formation might be solved if models took into account the increase of the solid surface density due to the interplay of the evaporation of icy planetesimals that moved interior to the snow line and the recondensation of water

from the diffusion of vapor back outward (CZ04). CZ04’s models suggest that the solid surface density could be enhanced by more than an order of magnitude in the region between ϖ_{SL} and $\varpi_{\text{SL}} + d\varpi_{\text{diff}}$, where ϖ_{SL} is the location of the snow-line and $d\varpi_{\text{diff}}$ is the diffusion length scale. This material could be used to grow the giant planet cores.

In this subsection, we test the above hypothesis with direct N -body calculations using a modified version of the code described in §3. In order to simply mimic evaporation and recondensation, this code removes any tracer particle that evolves to a heliocentric distance less than ϖ_{SL} and replaces it with a new tracer with a heliocentric distance (ϖ) chosen at random from a uniform distribution between ϖ_{SL} and $\varpi_{\text{SL}} + d\varpi_{\text{diff}}$. Note that we are overestimating the outward shift of material because physically this is a diffusion process which puts more material near ϖ_{SL} than our uniform distribution does. We set $\varpi_{\text{SL}} = 3.9$ AU, which is slightly interior to the initial inner edge of our planetesimal disk at 4 AU, and $d\varpi_{\text{diff}} = 1$ AU, in accord with the results of CZ04’s modeling. Since this new tracer represents objects condensing from the gas disk, we place it on a circular orbit with an inclination of $\frac{1}{2} \tan(z_s/\varpi)$.

Once a planetesimal evaporates, not all of its mass diffuses back to outside the snow-line and recondenses. To account for this we set the mass of the new tracer to ϵ times the mass of the original. The way to interpret this is to recall that each tracer particle actually represents N objects of radius r_p or r_f , depending on whether they are ‘planetesimals’ or ‘fragments’. By changing the mass of the tracer, we are effectively decreasing N . The values of r_p and r_f remain fixed during the simulation. For lack of a better constraint, we used $\epsilon = 0.75$ for our original series of runs. This is a conservative value (in the sense of promoting embryo growth) given that the original planetesimals in this region are probably less than half water ice.

We performed five simulations with $r_p = 10$ km and $r_f = 1, 3, 10, 30,$ and 100 km.

All other free parameters are the same as in Run A. Our results show trends very similar to the runs without evaporation. In the runs with $r_f \geq 30$ m, fragments build up in the embryos’ resonances, and the embryos are pushed inward. Unlike the previous runs where the embryos were pushed out of the simulation region, however, here the embryos migrated until most of their strong mean motion resonances were closer to the Sun than the snow-line. For example, the runs with $r_f = 100$ m and 30 m migrated so that the heliocentric distance of the 2:1 and 5:3, respectively, were slightly less than ϖ_{SL} , i.e. their semi-major axes were at 2.5 and 2.8 AU, respectively. Once this occurred, the embryos stopped growing. The most massive embryo in these simulations was only $7.1 M_{\oplus}$.

In the runs $r_f \leq 3$ m, the fragments are small enough that they sweep by the planets. Recall that there is very little growth in similar runs without evaporation. Here, only the inner embryo grows because it sits in the condensation region. For both of the runs that showed this behavior ($r_f = 1$ m and $r_f = 3$ m), the inner embryo grew to $10 M_{\oplus}$ in 3 million years. However, again only one core grew and thus these systems are not like the Solar System. In addition, even with evaporation/recondensation, the systems lost far more mass ($\sim 90 M_{\oplus}$) to the inner regions than accreted onto the planet. This indicates that ϵ is a critical factor in these simulations and recall that we used a conservative value for this. In a simulation with $\epsilon = 0.25$, the inner embryo had a mass of only $4 M_{\oplus}$ at the end of the calculation. This is probably more typical of what we should expect in more realistic situations.

Once again interesting things occur at $r_f = 10$ m. In this run, the evolution of which is shown in Fig. 11, we see many of the processes thus far discussed combine to form four large cores, and thus we now describe its evolution in detail. For the first 100,000 years, the embryos grow and spread. Fragments are being accreted mainly by the innermost embryo (Embryo 1) because it sits in the condensation zone and it grows to $19 M_{\oplus}$. Recall that

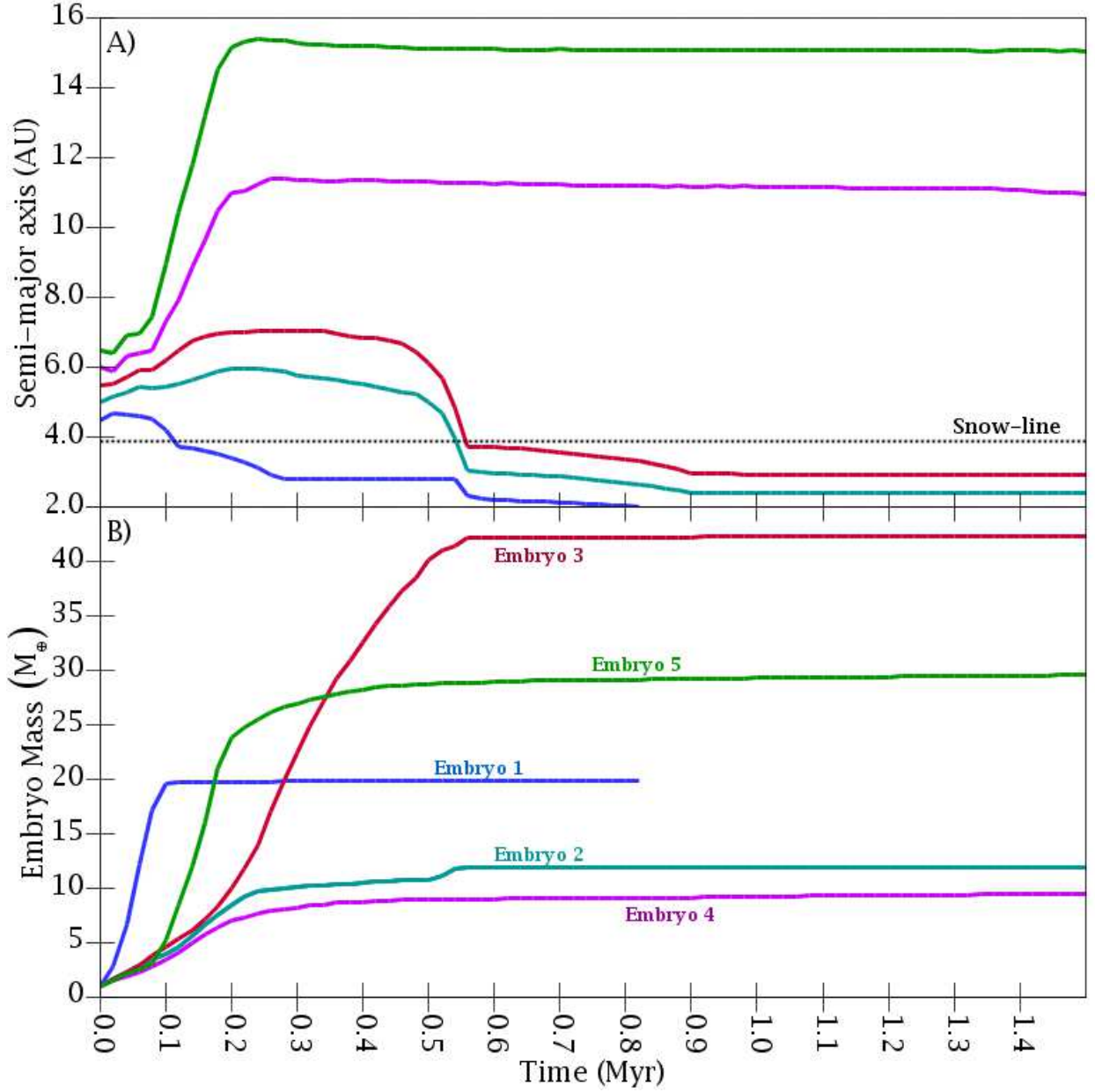


Fig. 11.— The temporal evolution of the five embryos in the evaporation run with $r_f = 10$ m, $r_p = 10$ km, and $\epsilon = 0.75$. A) The semi-major axes as a function of time. Each embryo is represented by a solid curve of a different color. The dotted line shows the assumed location of the snow-line. Embryo 1 falls out of the region that we simulate at 830,000 years. This is a numerical artifact, however. B) Embryo mass as a function of time. The color solid curves corresponds to the semi-major axes in (A).

we do not allow the embryos to accrete nebula gas or open gaps. Thus, from this time onward our simulation is missing physics that would potentially dominate the evolution. Having said this, the subsequent evolution supplies important insight into how the various processes interact, and so, we continue our description.

Between 80,000 and 230,000 years self-sustaining planetesimal migration causes the outer four embryos to migrate outward. During this time, the outermost (Embryo 5) grows to $26 M_{\oplus}$. As the embryos spread, fragments start to build up in the mean motion resonances of the Embryo 1. We believe that this occurs simply because the outward migration creates enough room between the two inner embryos to allow fragments to settle there. Embryo 1 starts to migrate inward and its growth stops. By 280,000 years its 5:3 mean motion resonance moves inside of the snow-line and it also stops migrating.

At this point, the action moves to the region between 8 and 11 AU. The self-sustaining outward migration left this region devoid of embryos and thus planetesimals start to concentrate there. As this occurs their collision rate is large and many fragments are formed. The fragments spiral in and are accreted by Embryo 3. Between 230,000 and 460,000 years, this embryo grows from 14 to $38 M_{\oplus}$. It is only at the end of this time that the embryo grows sufficiently large to trap the fragments in its exterior resonances. These fragments eventually push the inner three embryos toward the Sun. At 830,000 years Embryo 1 was pushed out of our simulation region. It had a mass of $20 M_{\oplus}$. The outer two embryos did not get pushed around by the fragments because their outward migration depleted the outer disk enough that the collision rate was small and so fragments did not form. At the end of the simulation there were four cores with masses ranging from 9 to $42 M_{\oplus}$. Presumably, the original Embryo 1 would also be present if we were not forced to remove it for technical reasons, as explained above.

We can only speculate as to how the system would have evolved if we had allowed the

embryos to directly accrete gas. All would have proceeded as before until Embryo 1 reached $\sim 10 M_{\oplus}$ at 60,000 years. We believe that this growth would not have stopped the onset of planetesimal driven migration, however. If it had any effect at all, it would have triggered the migration at an earlier time. Thus, Embryo 6 would have moved outward and also grown to the point where it would have accreted gas. The embryo reached $10 M_{\oplus}$ at 130,000 years in our simulation; at which point it was at 11 AU. It is unclear how the system would have behaved after this time. However, we believe that it is safe to conclude that we would have created two gas giant planets in this system — and in only 130,000 years. All this thanks to a combination of evaporation/recondensation and planetesimal driven migration.

5. Summary & Conclusions

We presented the results of a large number of N -body simulations of the formation of giant planet cores. Our goal was to measure the effectiveness of several mechanisms for enhancing overall growth rates. To achieve this, for most of our simulations we started with a simple system containing 5 Earth-mass embryos embedded near the inner edge of a planetesimal disk. This disk contained $200 M_{\oplus}$ of material that was spread from 4 to 16 AU. All the planetesimals were assumed to have the same radius r_p . Our simulations potentially included a combination of the following processes: 1) aerodynamic drag on the small-bodies, 2) collisional damping, 3) extended atmosphere around the embryos (Inaba and Ikoma 2003), 4) embryo eccentricity damping due to gravitational interaction with the gas disk, 5) fragmentation of the planetesimals to form objects with radius r_f , and 6) evaporation and recondensation at the snow line (Cuzzi & Zanhle 2004). Not all simulations employed all these processes. Our goal was to determine which of these processes would allow several $10 M_{\oplus}$ cores to form in less than 3 million years. Unless noted, these simulations assumed a gas disk with a surface density of 5 times the minimum mass solar nebula value

at 5AU, and varying in inverse proportion to heliocentric distance.

We first presented an example of the the most basic simulations we performed (Run A). In particular, it included Processes (1)–(4), but not (5) or (6). During this calculation the embryos quickly scattered planetesimals out of the region that they inhabited — forming two massive rings immediately adjacent to this region (see Fig. 3). The planetesimals became decoupled from the embryos due to the effects of aerodynamic drag. Very little growth occurred. This run illustrates the first major conclusion of this work — the gravitational interaction between the embryos and the planetesimals lead to the wholesale redistribution of material. Therefore, they must be handled in a realistic manner in order to produce reasonable results. This conclusion is true for all of our simulations.

Run A is representative of 90% of our simulations without fragmentation. The remaining 10%, however, exhibit quite dramatic behavior. In these simulations, we see a burst of outward migration. The outer embryos race through the distant disk, eating as they go. On timescales of the order of 120,000 years, the outer embryo can migrate ~ 6 AU and grow to roughly $30 M_{\oplus}$. In most of these simulations, several of the five embryos move outward and grow significantly. Indeed, in the example shown in Fig. 4 the cores have masses of between 3.2 and $29 M_{\oplus}$ by the end of the simulation.

Despite the success we have had with this so-called *planetesimal driven migration*, there is a problem — it occurred in only 10% of our simulations. However, we performed a set of simulations where we introduced 10 \sim Mars-mass embryos into the system. Although, there are some issues with these calculations (see §4.3), we see planetesimal driven migration in all cases. Thus, we believe that if we had been able to include a more realistic mass-distribution for the embryos, more of our systems would have exhibited this behavior.

We next performed a set of simulations which included the fragmentation of planetesimals. It was hypothesized that the creation of fragments would substantially

increase embryo growth rates because the fragments’ inclinations would quickly damp (due to their small sizes) and they would be in the shear-dominated regime when they encountered the embryos (Wetherill and Stewart 1993; R04). However, we found that this mechanism promotes rapid embryo growth only for a narrow range of parameters. In particular, for our nebular model, $r_f \leq 3$ m fragments were moving so quickly that they stream by the embryos without being accreted. For $r_f \geq 30$ m, the fragments pile up in mean motion resonances with the embryos rather than being accreted. Indeed, enough material gets trapped in the resonances that it can push the embryos into the inner Solar System (see Fig. 6).

Only for $r_f = 10$ m do we see a significant amount of growth. Indeed, for this narrow set of parameters, we produce cores larger than $10 M_\oplus$ by our 3 million year time limit. Unfortunately, we were unable to find a way to broaden the range of parameters over which this mechanism functions. Therefore, we are not very optimistic that this mechanism will prove valuable in the long run. Indeed, in most cases it did more harm than good.

Of particular concern is the fact that the fragments can get trapped in the mean motion resonances with the embryos and then push them around. We believe that our simulations show that icy planetesimals must break in such a way to avoid putting much mass in fragments with radii between ~ 30 m and ~ 1 km. Fortunately, there is observational evidence that supports this conclusion. In particular, we note that of the ≥ 50 asteroid families thus far discovered (Nesvorný et al. 2006), none are composed of what are believed to be the most comet-like asteroid types (P and D-types). This despite the fact that P and D-types make up at least 10% of known asteroids (Mothé-Diniz et al. 2003). Indeed, although $\sim 90\%$ of the Trojans asteroids are P/D-types, the only asteroid family in the swarms is a more normal C-type (M. Brož, pers. comm.). The simplest interpretation for these observations is that when a comet-like object breaks apart, it is pulverized to small

sizes. This is also supported by crater counts on the Galilean satellites, which show a dearth of primary impactors in the size range we are discussing (Bierhaus et al. 2005).

Finally, we did a set of simulations that modelled the evaporation of planetesimals at the snow-line (which we put at ~ 4 AU) and had them to recondense at random locations between 4 AU and 5 AU. This process will increase the surface density of solids in this region and thereby increase accretion rates. We find that in simulations with fragments radii greater than 30 m, the embryos are pushed inside the snow-line by resonant-trapped fragments and very little growth occurs. For $r_f \leq 3$ m, the fragments sweep by all but the innermost embryo. As a result, only the inner embryo grows. Although this can produce a core of $10 M_\oplus$, it is an inefficient process, and 90% of the fragments are lost to the inner Solar System. We performed one simulation with $r_f = 10$ m which produced a system with many cores more massive than $10 M_\oplus$. In this simulation, the growth of the innermost core triggered planetesimal driven migration in the rest of the embryos (see Fig. 11).

In summary, we find that widely used approximations for core accretion typically overestimate the ability of models to produce sufficiently large cores because they do not incorporate the dynamical influences which redistribute planetesimals near the feeding zones of the embryos. As a result of this, we believe that planetesimal driven outward migration offers the best hope for solving the issue of giant planet core formation. Clearly more work needs to be done to demonstrate its effectiveness. In particular, the effects of a realistic size distribution must be taken into account. This is computationally challenging and thus we leave it for future work.

This work has been directly supported by a grant from the National Science Foundation (Award ID 0708775). HFL is also grateful for funding from NASA’s Origins, and OPR programs. We would like to thank Bill Bottke, John Chambers, and Alessandro Morbidelli for useful discussions.

References

- Adachi, I., Hayashi, C., and Nakazawa, K.: 1976, *Progress of Theoretical Physics* **56**, 1756.
- Agnor, C.B., Canup, R.M., and Levison, H.F.: 1999, *Icarus* **142**, 219.
- Alibert, Y., Mordasini, C., Benz, W., and Winisdoerffer, C.: 2005, *Astron. Astroph.* **434**, 343.
- Benz, W., Asphaug, E. 1999. Catastrophic Disruptions Revisited. *Icarus* **142**, 5-20.
- Bierhaus, E. B., Chapman, C. R., Merline, W. J. 2005. Secondary craters on Europa and implications for cratered surfaces. *Nature* **437**, 1125-1127.
- Brasser, R., Duncan, M. J., Levison, H. F. 2006. Embedded star clusters and the formation of the Oort Cloud. *Icarus* **184**, 59-82.
- Capobianco, C., Duncan, M., and Levison, H.: 2009 in preparation
- Chambers, J. 2008. Oligarchic growth with migration and fragmentation. *Icarus* **198**, 256-273.
- Chambers, J.E. and Wetherill, G.W.: 1998, *Icarus* **136**, 304.
- Chambers, J.E.: 2001, *Icarus* **152**, 205.
- Cuzzi, J.N. and Zahnle, K.J.: 2004, *Astrophys. J.* **614**, 490.
- Durda, D. D., Bottke, W. F., Nesvorný, D., Enke, B. L., Merline, W. J., Asphaug, E., Richardson, D. C. 2007. Size frequency distributions of fragments from SPH/N-body simulations of asteroid impacts: Comparison with observed asteroid families. *Icarus* **186**, 498-516.
- Duncan, M.J., Levison, H.F., and Lee, M.H.: 1998, *Astronomical Journal* **116**, 2067.

- Fernandez J. A. and Ip, W.-H.: 1984, *Icarus* **58**, 109.
- Goldreich, P., Lithwick, Y., and Sari, R.: 2004a, *Annual Review of Astronomy and Astrophysics* **42**, 549.
- Goldreich, P., Lithwick, Y., Sari, R. 2004b. Final Stages of Planet Formation. *Astrophysical Journal* **614**, 497-507.
- Gomes, R.S., Morbidelli, A., and Levison, H.F.: 2004, *Icarus* **170**, 492.
- Hahn, J.M. and Malhotra, R.: 1999, *Astronomical Journal* **117**, 3041.
- Haisch, K.E., Jr., Lada, E.A., and Lada, C.J.: 2001, *Astrophys. J.* **553**, L153.
- Halliday, A.: 2004, *Nature* **431**, 253.
- Hayashi, C.: 1981, *Prog. Theor. Phys.* **70**, 35.
- Hayashi, C., Nakazawa, K., Nakagawa, Y. 1985. Formation of the solar system. *Protostars and Planets II* 1100-1153.
- Hillenbrand, L. A. 2008, *Physica Scripta Volume T*, 130, 014024
- Hubickyj, O., Bodenheimer, P., and Lissauer, J.J.: 2005, *Icarus* **179**, 415.
- Ida, S. and Makino, J.: 1993, *Icarus* **106**, 210.
- Inaba, S. and Wetherill, G.W.: 2001, *Lunar and Planetary Institute Conference Abstracts* **32**, 1384.
- Inaba, S. and Ikoma, M.: 2003, *Astron. Astroph.* **410**, 711.
- Inaba, S., Wetherill, G.W., and Ikoma, M.: 2003, *Icarus* **166**, 46.

- Kary, D. M., Lissauer, J. J., Greenzweig, Y. 1993. Nebular gas drag and planetary accretion. *Icarus* **106**, 288.
- Kirsh, D. R., Duncan, M., Brasser, R., Levison, H. F. 2009. Simulations of planet migration driven by planetesimal scattering. *Icarus* **199**, 197-209.
- Kokubo, E. and Ida, S.: 1998, *Icarus* **131**, 171.
- Kokubo, E. and Ida, S.: 2000, *Icarus* **143**, 15.
- Kominami, J., Tanaka, H., and Ida, S.: 2005, *Icarus* **178**, 540.
- Korycansky, D.G. and Pollack, J.B.: 1993, *Icarus* **102**, 150.
- Laughlin, G. and Adams, F.C.: 1997, *Astrophys. J.* **491**, L51.
- Levison, H. F., Duncan, M. J. 2000. Symplectically Integrating Close Encounters with the Sun. *Astronomical Journal* **120**, 2117-2123.
- Levison, H. F., Morbidelli, A. 2007. Models of the collisional damping scenario for ice-giant planets and Kuiper belt formation. *Icarus* **189**, 196-212.
- Levison, H. F., Morbidelli, A., Gomes, R., Backman, D. 2007. Planet Migration in Planetesimal Disks. *Protostars and Planets V* 669-684.
- Lissauer, J. J. 1987. Timescales for planetary accretion and the structure of the protoplanetary disk. *Icarus* **69**, 249-265.
- McNeil, D., Duncan, M., and Levison, H.F.: 2005, *Astronomical Journal* **130**, 2884.
- Mizuno, H.: 1980, *Progress of Theoretical Physics* **64**, 544.
- Mizuno, H., Nakazawa, K. and Hayashi, C.: 1978. *Prog. Theor. Phys.* **60**, 699.

- Mothé-Diniz, T., Carvano, J. M., & Lazzaro, D. 2003. Distribution of taxonomic classes in the main belt of asteroids. *Icarus* **162**, 10-21.
- Nesvorný, D., Bottke, W. F., Vokrouhlický, D., Morbidelli, A., Jedicke, R. 2006. Asteroid families. *Asteroids, Comets, Meteors* **229**, 289-299.
- Paardekooper, S.-J., Papaloizou, J. C. B. 2008. On disc protoplanet interactions in a non-barotropic disc with thermal diffusion. *Astronomy and Astrophysics* **485**, 877-895.
- Papaloizou, J.C.B. and Larwood, J.D.: 2000, *Monthly Notices of the Royal Astronomical Society* **315**, 823.
- Pollack, J.B., Hubickyj, O., Bodenheimer, P., Lissauer, J.J., Podolak, M., and Greenzweig, Y.: 1996, *Icarus* **124**, 62.
- Rafikov, R.R.: 2004, *Astronomical Journal* **128**, 1348.
- Raymond, S. N., Scalo, J., Meadows, V. S. 2007. A Decreased Probability of Habitable Planet Formation around Low-Mass Stars. *Astrophysical Journal* **669**, 606-614.
- Skeel, R. D., & Biesiadecki, J. J.: 1994, *Ann. Numer. Math.* **1**, 191.
- Stevenson, D.J. and Lunine, J.I.: 1988, *Icarus* **75**, 146.
- Touboul, M., Kleine, T., Bourdon, B., Palme, H., Wieler, R. 2007. Late formation and prolonged differentiation of the Moon inferred from W isotopes in lunar metals. *Nature* **450**, 1206-1209.
- Thommes, E.W., Duncan, M.J., and Levison, H.F.: 2003, *Icarus* **161**, 431.
- Thommes, E.W., and Duncan, M.J.: 2006, in *Planet Formation: Theory, Observations, and Experiments*, ed. H. Klahr and W. Brander (Cambridge: Cambridge University Press), 129.

Ward, W.R.: 1986, *Icarus* **67**, 164.

Ward, W.R.: 1997, *Icarus* **126**, 261.

Weidenschilling, S. J., Davis, D. R. 1985. Orbital resonances in the solar nebula -
Implications for planetary accretion. *Icarus* **62**, 16-29.

Wetherill, G.W. and Stewart, G.R.: 1989, *Icarus* **77**, 330.

Wetherill, G.W. and Stewart, G.R.: 1993, *Icarus* **106**, 190.

Wisdom, J. and Holman, M.: 1991, *Astronomical Journal* **102**, 1528.

Wisdom, J. and Holman, M.: 1991, *Astronomical Journal* **102**, 1528.

Zappalà, V., Cellino, A., dell’Oro, A., Paolicchi, P. 2002. Physical and Dynamical Properties
of Asteroid Families. *Asteroids III* 619-631.